State Water Survey Division

CLIMATOLOGY SECTION
AT THE
UNIVERSITY OF ILLINOIS

Illinois Department of
Energy and Natural Resources

Miscellaneous Publication 61

ILLINOIS SOLAR AND WIND CLIMATE

by

Keith Hendrie and Wayne M. Wend/and

Champaign, Illinois

December 1981

INTRODUCTION

The potential resource of solar and wind energy over the area of Illinois is indeed great. The percent of total demand which may be realized from these two "renewable" energy sources depends on the maximum potential, and the efficiency with which the energy is captured. The first of these two concerns is addressed in the following pages.

Over Illinois, solar energy reaches a maximum value during the summer, whereas wind power reaches its annual maximum in late winter and spring. If energy is extracted from both sources, a greater potential energy demand may be satisfied during more months of the year (the least probability of extracted energy being late fall and early winter).

Unfortunately on the diurnal cycle, the potential of wind energy at night decreases to about half its daytime value, and of course, there is no potential of solar energy at night, unless some storage mechanism is employed.

SOLAR RADIATION

One of the most obvious renewable energy sources that can be utilized in our attempts to develop alternative energy supplies in an effort to relieve our dependence upon imported petroleum supplies is solar energy. However, if an effective solar energy program is to be achieved, we must develop an economically viable solar technology, and this requires a good knowledge of the characteristics of the solar radiation incident at the surface, and its spatial, temporal, and weather-related variations. It is also important to be aware of any long-term trends in the intensity and characteristics of the solar energy being received at the surface, and the impact of urban and industrial development upon it.

Factors Influencing the Receipt of Solar Radiation at the Surface

A number of factors are involved, some resulting in a systematic pattern to the variations, and others providing a quite variable pattern superimposed over these known and predictable differences. The systematic variations are due to astronomical factors resulting from earth-sun relationships, and include the rotation of the earth on its axis, the inclination to the plane of the ecliptic and parallelism of the earth's axis as it revolves about the sun, the fact that the earth's orbit is actually slightly elliptical, and the spherical shape of the earth's surface. The other more random variations result from a number of factors which impinge upon the incoming solar beam causing depletion by absorption, reflection back to space and/or scattering, or alter its characteristics. These factors include the optical path length through the atmosphere, cloud type and cover, concentrations of atmosphere gases such as water vapor, ozone and oxygen, nature and concentration of atmospheric particulates, slope and aspect of the surface, topography, and reflectivity of the surface.

The rotation of the earth on its axis results in day and night and a consequent diurnal and discontinuous pattern of solar energy received at the surface with a diurnal peak receipt at solar noon if all other factors remain constant. This leads directly to one of the major problems confronting the solar power concept; that of redistribution of the energy captured over the whole day in a more temporally equitable manner, or in fact even providing more at night when energy demand often peaks.

The inclination of the earth's axis at 66 1/2° to the plane of the ecliptic and its constancy of orientation in space as the earth revolves about the sun, causes a seasonal pattern in the solar radiation incident at any one point on the surface. The mean daily solar elevation of the direct solar beam at any one point changes continually through the year with a cycle covering a range of 47°, and thus at solar noon, an appropriately tilted surface is a more efficient collector since it maximizes the incident solar flux density at that time. By reference to Table 1, it can be seen for Illinois that as an annual mean, a south-facing reflector tilted at 40° from the vertical is most efficient at noon. However, the angle of tilt could be varied seasonally and N-S across the state to be more efficient, and on a diurnal basis it is not the most efficient collector orientation at all times due to the changing aximuth. This seasonal effect also results in a variation in daylength which in turn has significant inplications for the adoption of a solar energy program. Data in Table 1 indicates a mean annual change in daylength for Illinois of almost 6 hours, with the shortest daylength being in early to mid-winter when a peak energy demand exists.

Table 1. Solar elevation (θ°) at noon and annual variation in daylength (hr:min) for Illinois during equinoxes and solstices.

	Extreme South	Central	Chicago
θ at winter solstice (December 22)	13 1/2	16 1/2	18 1/2
θ at vernal and autumnal equinoxes (March 21, September 23)	37	40	42
θ at summer solstice	60 1/2	63 1/2	65 1/2
Annual variation in daylength	5:12	5:41	6:08

On a global basis the elliptical shape of the earth's orbit results in hemispherical differences, since the earth is closer to the sun during summer in the southern hemisphere and further from it during summer in the northern hemisphere.

The spherical curvature of the earth's surface also causes a latitudinal variation in receipt of solar energy because it results in a latitudinal variation in the incident flux density at any point in time (See Figs. 1 and 2 for this effect on Illinois). As solar elevation decreases (or zenith angle increases) the same amount of solar energy impinges on a larger surface area, thereby being less intense. In the absence of other factors, the incident flux density (θ_z) varies with the cosine of the zenith angle (z) as

$$\Theta_z = \Theta_o \cos z$$

where θ_o is the flux density on a surface to which the solar beam is normal, This effect also provides much of the explanation for the seasonal and diurnal variations in receipt of solar radiation, with minimum intensities during winter and early/late in the day being due largely to the greater zenith angle at these times.

Another factor reinforces this geometric effect of changing zenith angle. As the zenith angle increases (or solar elevation "decreases), so the optical pathlength of the solar beam through the atmosphere increases. This means that there is greater attenuation of the solar beam by scattering, reflection, and absorption due to the greater chance of interception by clouds, aerosols, atmospheric gases and particulates, thereby further reducing the solar intensity at the surface during winter and early/late in the day.

The attenuation of the solar beam due to its interception by clouds, aerosols, gases and particulates has a number of effects, all of which are highly variable due to the wide differences in concentration and nature of most of the intercepting agents in both space and time, and which are governed mainly by meteorological processes. Firstly, it considerably reduces the energy received at the surface compared to that received at the top of the atmosphere by the reflection and scattering of some of it straight back to space. It also results in changes in the nature of the solar beam from a totally direct beam at the top of the atmosphere, to global radiation, being a combination of direct and diffuse components, which is received at the surface. On clear days in Illinois, typically the diffuse component comprises about 20% of the total in mid-summer and about 35% of the total in mid-winter. These percentages increase considerably in the presence of haze and cloud. The ratios of direct to diffuse components become important with solar collectors which depend upon concentration of the solar beam, since they are sensitive mainly to the direct fraction. Additionally, a cloud cover reduces the total global radiation received at the surface. The third effect is to change the spectral composition of the incoming radiation. Under clear skies the spatial composition of global radiation is about 6% ultraviolet, 47% visible wavelengths, and 47% infrared. Under cloudy skies there is a reduction in the infrared portion of the spectrum and the visible section may then account for 50+%.

Data Availability and Accuracy

At the present, solar radiation data are being measured at a number of places in Illinois, but direction of operations at these sites lacks coordination, and they are not of sufficiently compatible form to incorporate their data into one picture for a number of reasons. Often these measurements are being made for a relatively short period of time and with widely different objectives which bear strongly on the methodology adopted. In most cases the acquisition of data has commenced very recently, meaning that little value can be attributed to them as being representative of any mean value. Additionally, the type of instrumentation employed varies widely, resulting in a variety of differences in the sensor outputs related to the instrument characteristics, mounting and exposure, and resulting in incompatible data in many cases. The types of factors involved here can lead to wide variations in calibrated output, often of the order of 10-20%, and under certain conditions much greater. These factors include differences in instrument response time, varying instrument sensitivity to temperature, spectral composition of the incoming radiation, aximuth, orientation and zenith angle, and also changing sensitivities when instruments are mounted in non-horizontal positions. The procedures adopted for instrument calibration and maintenance also vary widely, and the nature of the exposure, particularly in the case of tilted sensors, lacks consistency.

Hence, in view of the potentially large uncertainties, it was decided to consider only data from the sparse national network which is, however, governed by a consistent policy of instrumentation type, calibration, maintenance, and methodology, and to supplement these data with estimates obtained for other locations, and based upon parameters such as cloudiness. Since

Table 2. Monthly mean values of derived or mensured daily total global radiation received on a horizontal surface (BTU It^{-2}) and daily global k_t cloudiness index. (From Knapp et al., 1980.)

Month	Chicago, IL *	Moline, IL *	Spring-field, IL *	Evans-ville, IN *	Indian-apolis, IN M	South Bend IN *	Burling-ton, IA *	Louis-ville, KY *	Columbia MO M	St. Louis MO *	Nash-ville, TN M	Madison WI M	Milwaukee WI *
(1) Monthly means of daily total global radiation (BTU ft^{-2}):													
Jan	507.0	535.1	584.7	574.1	495.6	415.7	579.2	545.5	611.5	627.4	576.6	515.2	479.4
Feb	759.5	812.0	860.9	823.2	746.9	659.6	858.6	789.3	874.8	885.6	823.8	804.0	736.5
Mar	1106.9	1118.6	1143.0	1151.0	1037.4	992.5	1165.1	1102.0	1178.8	1204.7	1129.8	1136.0	1088.8
Apr	1459.0	1459.5	1515.0	1500.8	1398.4	1387.4	1537.9	1466.7	1525.9	1564.2	1543.6	1398.4	1442.7
May	1788.9	1753.9	1865.5	1782.8	1688.0	1722.5	1875.6	1719.8	1879.8	1871,3	1824.8	1743.2	1768.4
Jun	2007.0	1969.4	2096.7	1982.7	1868.1	1921.9	2121.0	1903.5	2089.5	2092.5	1963.5	1947.9	1977.1
Jul	1943.8	1938.6	2058.2	1920.3	1806.3	1852.4	2084.9	1837.5	2116.1	2049.5	1891.1	1934.4	1961.8
Aug	1719.4	1714.6	1805.8	1735.1	1643.5	1666.3	1828.1	1680.2	1877.9	1816.5	1736.9	1708.1	1719.0
Sep	1353.9	1357.0	1453.9	1403.3	1324.0	1291.3	1416.5	1361.2	1450.4	1459.2	1397.9	1299.4	1310.3
Oct	968.9	995.9	1068.3	1087.0	977.0	909.2	1060.8	1042.2	1100.8	1099.8	1113.8	910.9	907.9
Nov	565.5	594.6	676.6	682.5	579.1	497.1	663.7	652.8	702.7	718.3	711.3	504.2	524.6
Dec	401.5	432.9	490.1	498.7	416.6	340.3	480.7	487.9	522.5	530.6	520.6	388.9	378.4
Ann	1215.1	1223.6	1301.5	1261.8	1165.0	1138.0	1306.0	1215.7	1327.6	1326.6	1269.7	1190.9	1191.2
(2) Monthly mean values of the dally global k_t cloudiness Index:													
Jan	0.402	0.419	0.428	0.392	0.361	0.329	0.440	0.374	0.430	0.440	0.369	0.434	0.401
Feb	0.439	0.465	0.470	0.429	0.407	0.380	0.482	0.413	0.465	0.470	0.409	0.484	0.441
Mar	0.464	0.467	0.464	0.454	0.421	0.416	0.481	0.436	0.471	0.481	0.433	0.488	0.466
Apr	0.481	0.480	0.491	0.481	0.453	0.457	0.503	0.470	0.491	0.503	0.488	0.466	0.480
May	0.511	0.500	0.530	0.505	0.480	0.492	0.534	0.487	0.533	0.531	0.516	0.499	0.506
Jun	0.542	0.532	0.566	0.536	0.505	0.519	0.573	0.515	0.565	0.566	0.532	0.526	0.534
Jul	0.539	0.537	0.570	0.531	0.500	0.514	0.578	0.508	0.586	0.567	0.523	0.537	0.545
Aug	0.533	0.530	0.554	0.528	0.504	0.516	0.563	0.511	0.573	0.554	0.524	0.533	0.536
Sep	0.511	0.510	0.536	0.506	0.487	0.487	0.528	0.492	0.528	0.531	0.494	0.499	0.502
Oct	0.489	0.499	0.516	0.505	0.470	0.458	0.523	0.485	0.520	0.518	0.497	0.475	0.472
Nov	0.402	0.417	0.447	0.425	0.381	0.352	0.454	0.408	0.449	0.457	0.416	0.377	0.390
Dec	0.355	0.377	0.396	0.373	0.335	0.300	0.405	0.367	0.404	0.409	0.361	0.368	0.355
Ann	0.492	0.493	0.514	0.487	0.459	0.460	0.522	0.470	0.517	0.517	0.480	0.491	0.489

M Data derived from corrected hourly solar radiation measurements (1952-1975).
* Data derived from empirical relationships of cloudiness with measurements of solar radiation at other stations.

none of these stations are in Illinois, the four closest (Madison, WI; Columbia, MO; Nashville, TN; Indianapolis, IN) were used, and their data were supplemented with records from the Argonne National Laboratories, Lemont, IL which were considered comparable, and were available from September 1950 to the present. Unfortunately due to calibration problems in the past, the data for Urbana were not considered sufficiently reliable to be included in the analysis. To supplement these measured values, empirically derived data, based upon relationships between global radiation and cloudiness, were included for a number of other locations in and around the state (Chicago, IL; Moline, IL; Springfield, IL; Evansville, IN; South Bend, IN; Burlington, IA; Louisville, KY; St. Louis, MO; and Milwaukee, WI).

Data for these locations representing the period 1952-1975 are listed as monthly and annual means of total global (direct and diffuse) radiation in Tables 2 and 3.

Table 3. Monthly and annual means of daily total global radiation received on a horizontal surface at Lemont, IL (Argonne National Laboratory) for the periods 1950-1978, 1950-1964, and 1966-1978 (BTU ft^{-2}).

	J	F	M	A	M	J	J	A	S	0	N	D	Year
1950-1978	596	854	1145	1440	1790	2010	1944	1729	1396	996	588	460	1244
1950-1964	601	856	1163	1470	1858	2104	1973	1785	1500	1049	635	498	1289
1966-1978	585	852	1125	1408	1716	1910	1914	1668	1275	935	534	416	1196

The limits of accuracy of the data from the measurement stations (marked M in Table 2, plus Lemont in Table 3) should be better than ±5% at the 95% level of confidence for those particular locations, depending upon instrument maintenance. The empirically derived data (for stations marked * in Table 2)

Table 4. Useful unit conversion factors.

	TO CONVERT	TO	MULTIPLY BY
ENERGY	BTU	kWh	2.931×10^{-4}
	BTU	k cal	2.520×10^{-1}
	BTU	J	1.055×10^{3}
	kWh	k cal	8.600×10^{2}
	kWh	MJ	3.600
	k cal	J	4.186×10^{3}
ENERGY FLUX (Power)	BTU h^{-1}	kW	2.931×10^{-4}
	BTU h^{-1}	k cal min^{-1}	4.200×10^{-3}
	BTU h^{-1}	W (=Js^{-1})_	2.931×10^{-1}
	kW	k cal min^{-1}	1.433×10
	k cal min^{-1}	W	6.977×10
ENERGY FLUX DENSITY	BTU ft^{-2} h^{-1}	Wm^{-2}	3.155
	BTU ft^{-2} h^{-1}	kJm^{-2} h^{-1}	1.141
	BTU ft^{-2} h^{-1}	MJm^{-2} d^{-1}	2.739×10^{-2}
	BTU ft^{-2} h^{-1}	ly h^{-1}	2.726×10^{-2}
	BTU ft^{-2} h^{-1}	ly d^{-1}	6.542×10^{-1}
	ly h^{-1}	Wm^{-2}	1.163×10
	ly h^{-1}	kJm^{-2} h^{-1}	4.186×10
	ly h^{-1}	MJm^{-2} d^{-1}	1.005
	ly h^{-1}	cal cm^{-2} h^{-1}	1.000
	TO DERIVE	FROM	DIVIDE BY

will be quite variable in quality, both from station to station, and through the year, but the limits of accuracy should fall within the range of ±15-20% on average for those stations at the same level of confidence. Interpolation of data for other points (as from Figures 1 and 2) could involve considerable uncertainties, but in most cases should lie within ±25% of the estimation at the 95% level of confidence. The degree of uncertainty associated with the data presented, and which exists in much of the data currently being collected, amplifies the need for the state-wide solar monitoring network currently being established by the State Water Survey if we are to make economically sound decisions in the implementation of solar technology.

The units employed in this section have been based upon the BTU for energy, BTU h^{-1} for energy flux, and BTU-ft^{-2} h^{-1} for energy flux density. Since other units are often encountered in relation to solar energy, some useful conversion factors have been included in Table 4.

Distribution and Variation of Global Radiation Over Illinois

Figures 1A and 1B provide tentative spatial patterns of mean monthly global radiation received on a horizontal surface over the state and Figure 2 provides comparable annual mean data. Once data from the state solar monitoring network become available these relatively simple patterns will become modified, and with the more reliable data some changes could become quite significant.

A latitudinal gradient in solar radiation exists for all months, with lowest values in the north. Additionally, all months, and particularly January through September, exhibit a west to east decrease in solar input in response to the increase in cloudiness over the region as you move eastwards away from

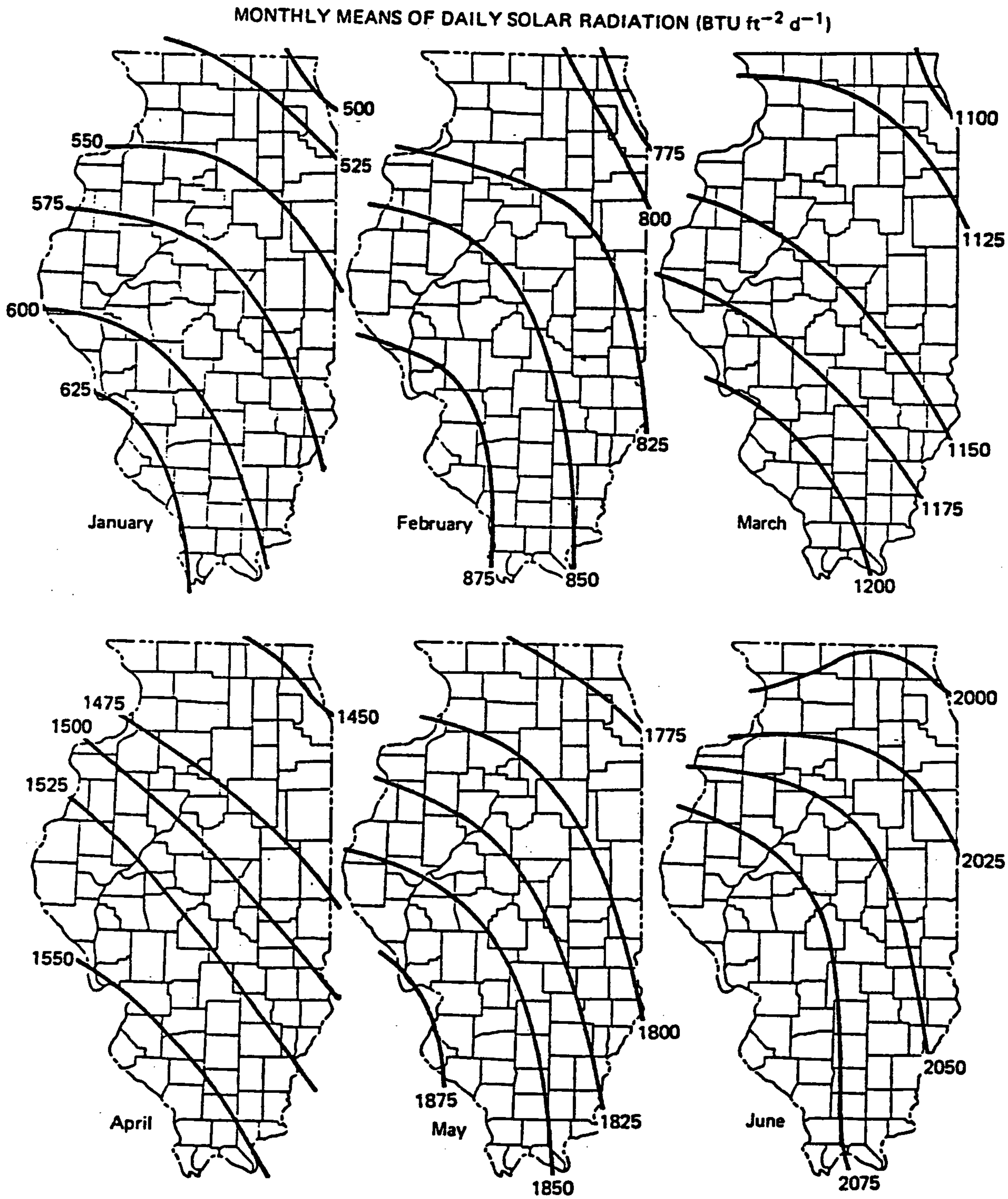
MONTHLY MEANS OF DAILY SOLAR RADIATION (BTU ft^{-2} d^{-1})
January
500
525
550
575
600
625
February
775
800
825
850
875
March
1100
1125
1150
1175
1200
April
1450
1475
1500
1525
1550
May
1775
1800
1825
1850
1875
June
2000
2025
2050
2075

Figure 1A

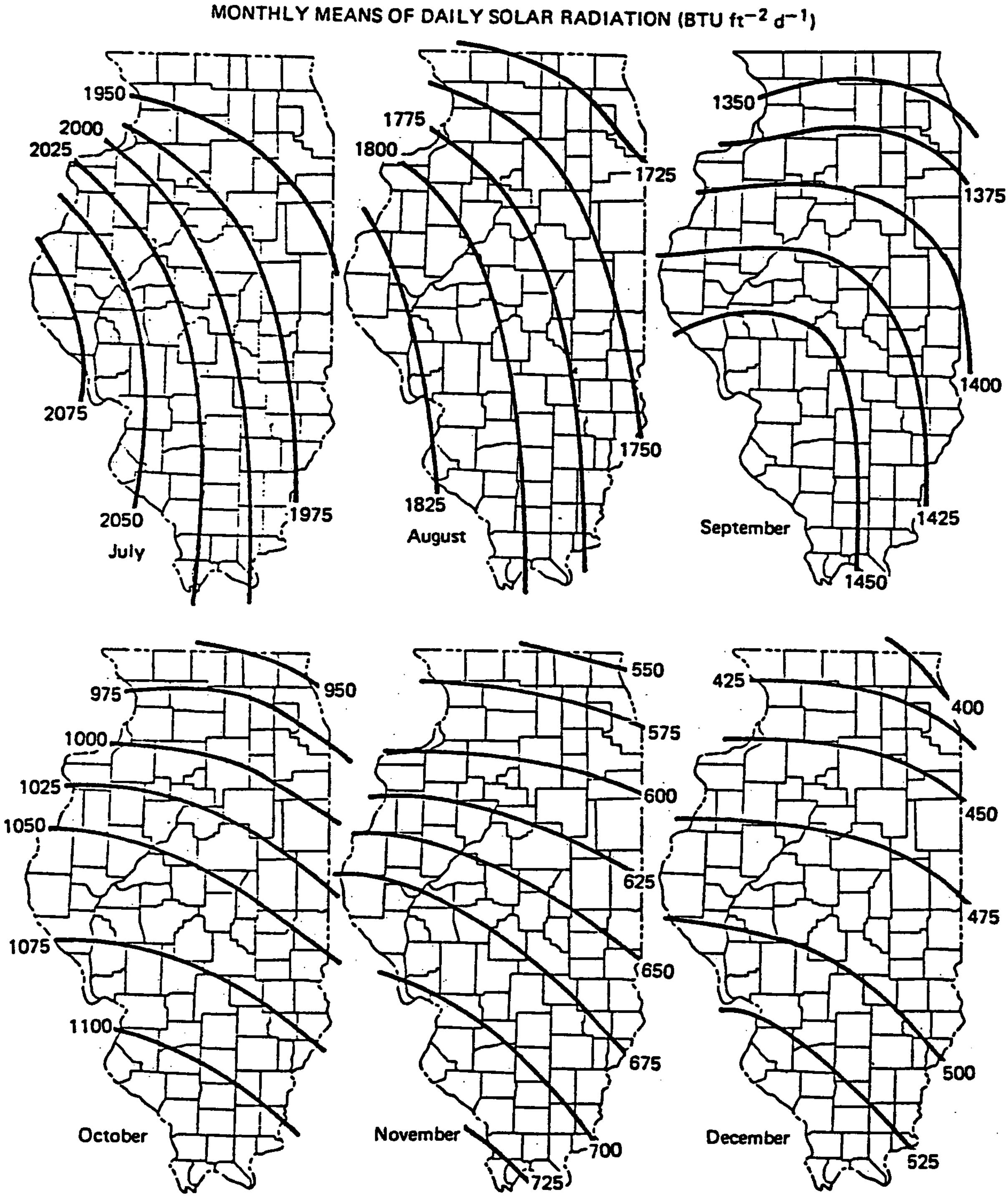
MONTHLY MEANS OF DAILY SOLAR RADIATION (BTU ft−2 d−1)
1950
2000
2025
2075
2050
1975
July
1775
1800
1725
1750
1825
August
1350
1375
1400
1425
1450
September
975
950
1000
1025
1050
1075
1100
October
550
575
600
625
650
675
700
725
November
425
400
450
475
500
525
December

Figure 1B

ANNUAL MEAN OF DAILY SOLAR RADIATION

(BTU ft^{-2} d^{-1})

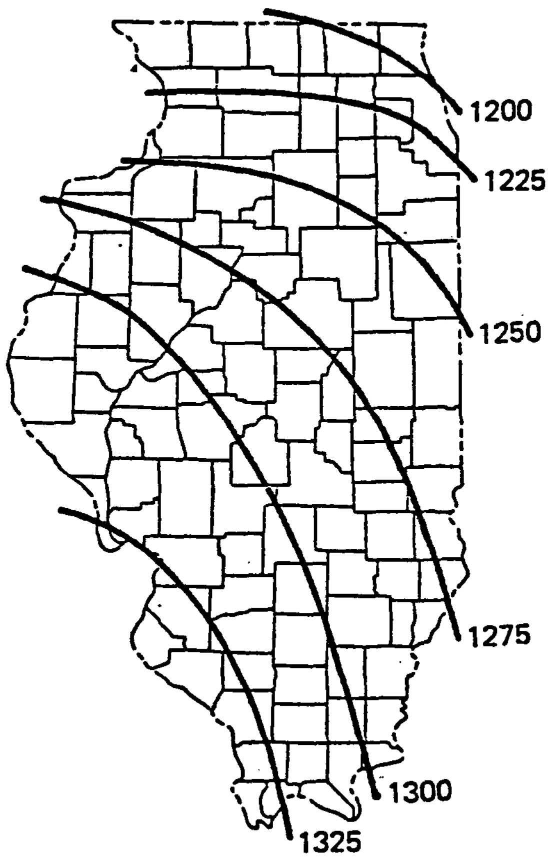

Figure 2

the Mississippi River. Also in the northeast there is a distinct minimum in solar energy related to increased cloudiness associated with Lake Michigan and the urban and industrial influence of the greater Chicago area.

Figure 3 provides monthly mean, extreme and percentile values of solar radiation received on a horizontal surface at Lemont, SW of Chicago. While this data cannot yet be provided for other areas of the State, it does give an estimate of the likely variability in monthly means of daily values. Mean monthly and annual data, both measured and empirically estimated, are listed for a number of stations in Tables 2 and 3.

Figure 4 shows the 10th, 25th, 50th, 75th, and 90th percentile values of monthly partitioned hourly solar radiation received on a horizontal surface at Lemont. The 10th percentile curve indicates the values below which 10% of all cases fell, or that were exceeded on 90% of all cases. The other precentile curves have similar meaning, with the 50% curve also representing the median value. These graphs clearly illustrate the diurnal and seasonal variations with maxima at noon, and in early to mid-summer. They also indicate the greater variability which seems to occur in March through May, and which is also apparent on Figure 3. Further, there are intersting effects of cloud cover patterns for April through July shown on the 10th and 25th percentile curves which include most of the data for days exhibiting convective and thick clouds. The time of major impact appears to become earlier in the day as one progresses through the months, being afternoon in April and from about 0900 to just after noon in July. This will obviously have implications for the collection of solar energy in the Chicago area, and indicates the need for detailed study of the problem.

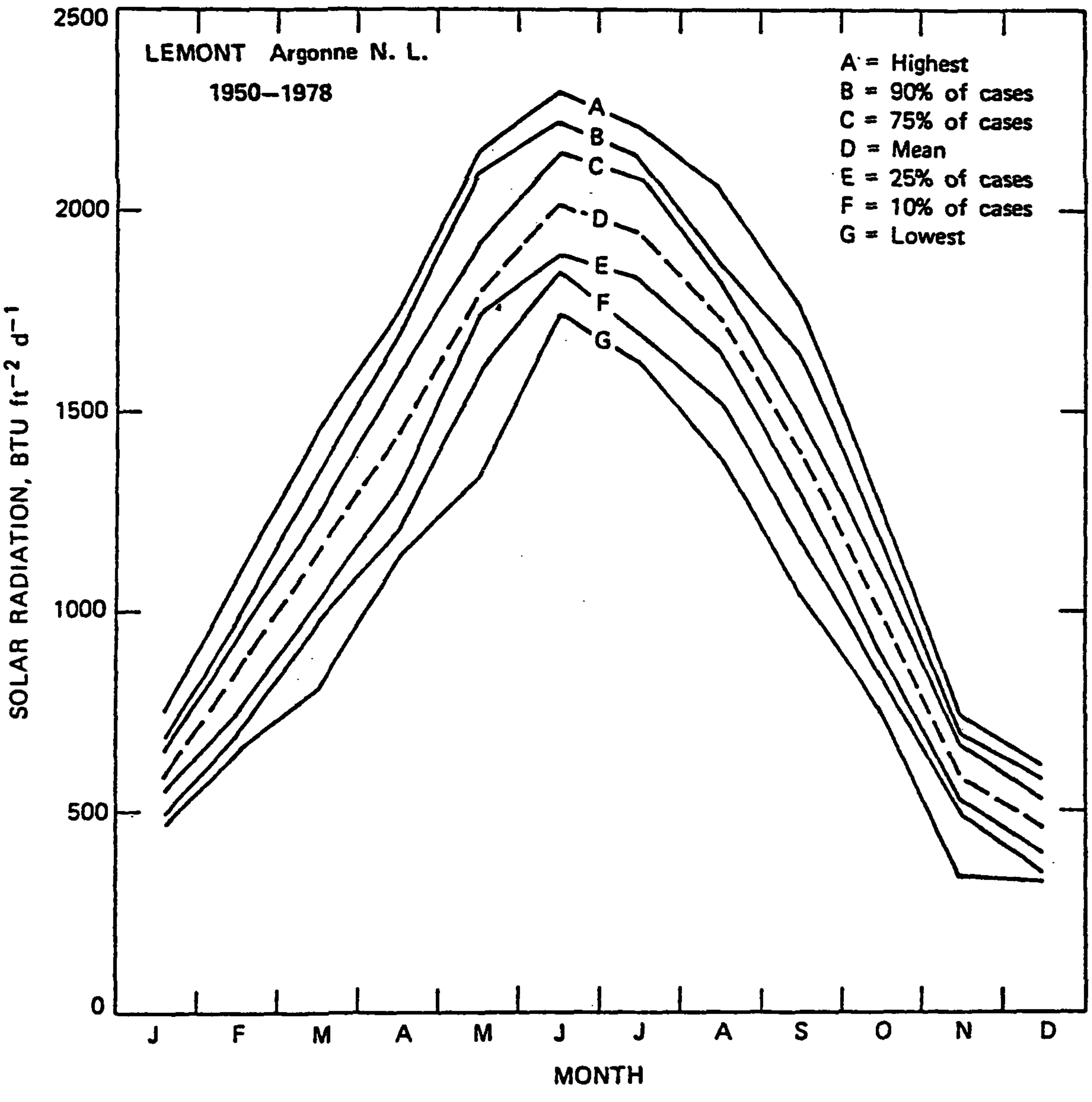
LEMONT Argonne N. L.
1950–1978
A = Highest
B = 90% of cases
C = 75% of cases
D = Mean
E = 25% of cases
F = 10% of cases
G = Lowest
A
B
C
D
E
F
G
2500
2000
1500
1000
500
0
SOLAR RADIATION, BTU ft^{-2} d^{-1}
J
F
M
A
M
J
J
A
S
O
N
D
MONTH

Figure 3

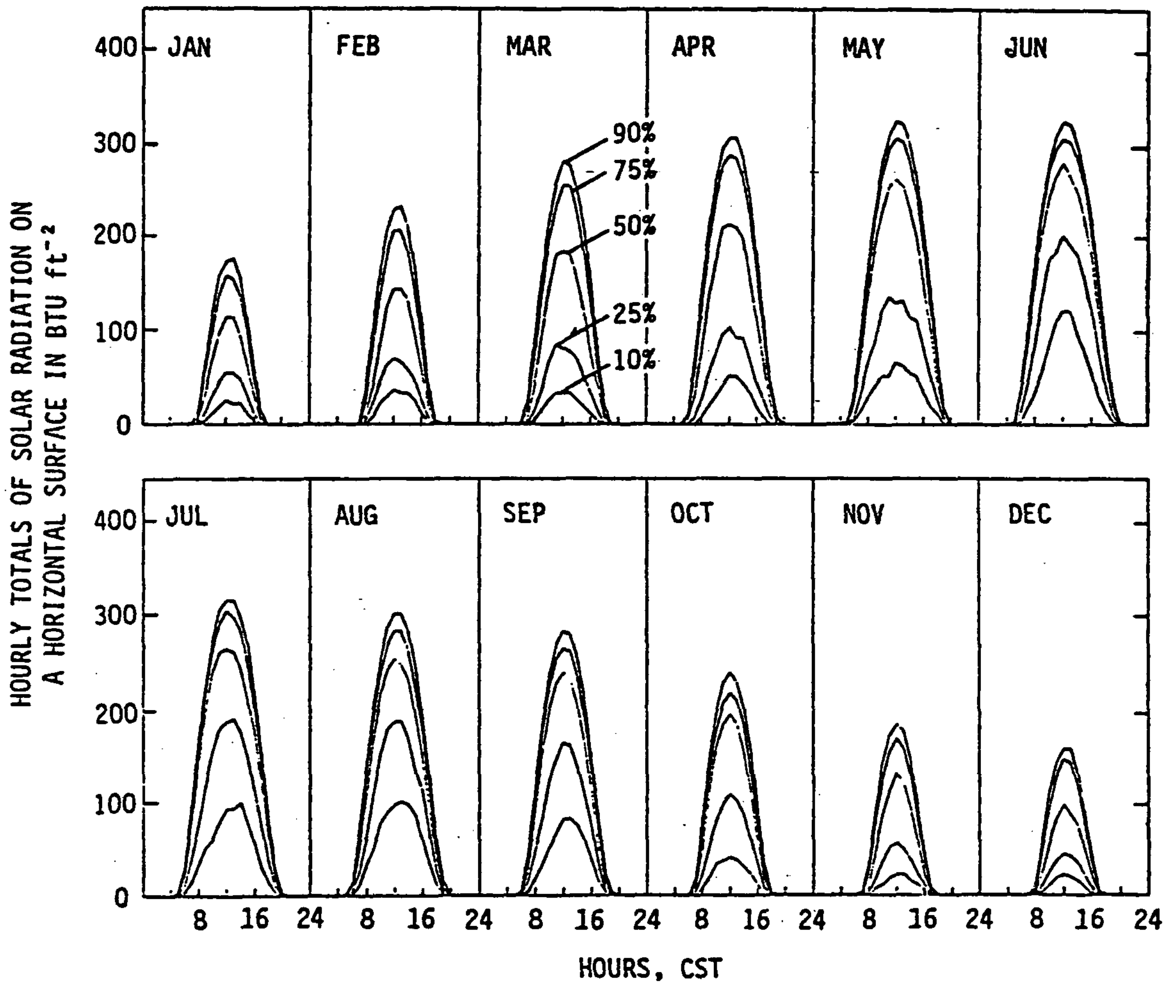
JAN
FEB
MAR
APR
MAY
JUN
JUL
AUG
SEP
OCT
NOV
DEC
90%
75%
50%
25%
10%
0
100
200
300
400
8
16
24
HOURLY TOTALS OF SOLAR RADIATION ON
A HORIZONTAL SURFACE IN BTU ft^{-2}
HOURS, CST

Figure 4

In the absence of available measurements of global radiation, daily or monthly estimates can be made by using simple empirical equations of the type:

$$Q = Q_A \, (a + b \, n/N)$$

where Q =global radiation on horizontal surfaces;

Q_A =extraterrestrial radiation impinging on the top of the atmosphere (in same units as Q);

n =hours of bright sunshine;

N =maximum possible hours of bright sunshine;

a, b =regression coefficients — vary with site and season, but approximate values for Illinois are:

a = 0.18 to 0.20: b = 0.50 to 0.55.

There are alternate, more sophisticated models becoming available, but they require detailed discussion and have not been included.

Estimating the Direct and Diffuse Components of Global Radiation

One of the most difficult problems involved in the utilization of solar radiation data for solar technology is the partitioning of the solar beam into its direct and diffuse compenents. For any given location this can be done either by measurement or by modeling.

Currently there is little reliable data available for Illinois, although some measurements are being made at the Argonne National Laboratories. Measurement of the direct beam involves solar tracking, and the equipment is both expensive and requires constant attention to maintain it in appropriate orientation. Measurement of the diffuse component involves shading of the sun from the instrument sensor, with need for correction for both other areas of the sky which are shaded and for internally reflected radiation impinging on the sensor, requiring a number of simplifying assumptions.

Modeling of the two components requires a good knowledge of the physical and optical characteristics that give rise to the scattering and reflection that results in the diffuse input. At the moment really adequate modeling of the proportionate contribution of each component has not been achieved, although SERI (Solar Energy Research Institute, Golden, CO) has a team of researchers tackling the problem. The simple models available at present are usually based upon the assumption that the diffuse component derives mainly from clouds in addition to some baseline value that always occurs, usually varying with solar elevation. Examples are given below:

(1) Short time periods (e.g., hourly)

$$q = 0.78 + 1.07\,\theta + 61.7C \qquad (1)$$

from Kreider and Kreith (1975);

where q = diffuse radiation received on a horizontal surface (BTU $ft^{-2}\ h^{-1}$)

θ = solar elevation (^{o})

C = cloud cover in tenths (0.0 = clear; 1.0 = totally overcast).

This is a computationally simple model that has fairly minimal data input requirements.

(2) Daily values

$$q = (Q+q)(1.0045+0.04349K_T-3.5227K_T^{2}+2.6313K_T^{3});$$

$$K_T \leq 0.75 \qquad (2a)$$

$$q = 0.166\,(Q+q);\ K_T > 0.75 \qquad (2b)$$

from Kreider and Kreith (1980);

where q = daily diffuse radiation received on a horizontal surface (BTU $ft^{-2}\ h^{-1}$);

Q = daily direct radiation received on a horizontal surface (BTU ft^{-2} h^{-1});

$Q+q$ = daily global radiation received on a horizontal surface (BTU ft^{-2} h^{-1});

K_T = daily clearness index;

and

$$K_T = \frac{(Q+q)}{Q_A} \tag{2c}$$

where Q_A = the daily extraterrestrial radiation received at the top of the atmosphere (BTU ft^{-2} h^{-1}).

This is a better formulation that (1) but is more demanding in its input requirements. There must be global radiation data and computation of K_T which necessitates values of Q_A; these can be obtained either from tables (e.g., Smithsonian Meteorological Tables, 1965) or determined computationally (after Sellers, 1965 and Stoffel, 1980) according to

$$Q_A = \frac{24}{\pi} s_o \left(\frac{\bar{r}}{r}\right)^2 (\omega_s \sin\phi \sin\delta + \cos\phi \cos\delta \sin\omega_s)$$

where s_o = solar constant (437 BTU ft^{-2} h^{-1});

$\bar{r}$ = mean distance of the sun from the earth;

r = actual distance of the sun from the earth on a particular day;

ω_s = sunset hour angle;

ϕ = station latitude;

δ = solar declination;

and

$$\delta = 0.006918 - 0.3999912 \cos\beta + 0.070257 \sin\beta - 0.006758 \cos 2\beta + 0.000907 \sin 2\beta - 0.002697 \cos 3\beta + 0.001480 \sin 3\beta$$

(in radians)

$$\left(\frac{\bar{r}}{r}\right)^2 = 1.00011 + 0.034221 \cos\beta + 0.001280 \sin\beta + 0.000719 \cos 2\beta + 0.000077 \sin 2\beta$$

where $\beta = \frac{2\,d}{365}$

and d = number of days in year minus one.

(3) Monthly values

$$q = (Q+q)\ (1.390-4.027\ \overline{K_T} + 5.531\ \overline{K_T}^2 - 3.108\ \overline{K_T}^3) \qquad (3a)$$

where the symbols have the same meaning as in (2) above, but are monthly values,

and

$$\overline{K_T} = \frac{(Q+q)}{\overline{Q}_A} \qquad (3b)$$

where $\overline{Q}_A$ = monthly mean extraterrestrial radiation received at the top of the atmosphere.

This provides monthly values of the diffuse component, and estimated values of $\overline{K_T}$ have been listed in Table 2 for the stations presented.

(4) Estimation of the direct component

An estimate of the direct component can be obtained simply by subtracting the diffuse estimate from the global radiation as:

$$Q = (Q+q) - q \qquad (4)$$

Solar Energy Receipt on Non-Horizontal Surfaces

While a horizontal surface provides the most appropriate reference orientation for obtaining comparable measurements at different sites, in most cases it is not the most efficient collecting surface orientation. In fact surfaces in any fixed orientation fail to provide the most effective surface of receipt since both solar elevation and azimuth (together provide a fix of the sun's position relative to the earth) continually change through the day, and in addition mean solar elevation changes through the seasons.

At any given time the most effective collecting surface is one which is oriented so that the direct solar beam is normal to it. Consequently the surface that would receive the greatest energy flux density is one which "tracks" the sun. However, this is prohibitively expensive in most cases, and so the most efficient collector that is economically viable for Illinois is one which is in a fixed mount, with its receiving sourface southfacing and tilted at about 40° (see Table 1). A simple improvement can be effected by providing the option of a monthly or seasonal adjustment of the tilt angle.

To compute the instantaneous intensity of the direct component of the incident solar radiation on surfaces of different orientation, the following equations can be used.

(1) for a horizontal surface --

$$Q_H = Q_O \cos Z;$$

(2) for a vertical surface --

$$Q_V = Q_O \sin Z \cos (a-a_o);$$

(3) for sloping surfaces other than vertical --

$$Q_S = Q_O (\text{Cos } Z \text{ Cos } S + \sin Z \sin S \cos (a-a_o)];$$

where Q_H, Q_V, and Q_S are the instantaneous fluxes of direct beam solar radiation on horizontal, vertical and sloping surfaces, respectively.

Q_O = the intensity of the direct beam on a surface normal to the sun's rays;

Z = the zenith angle of the solar beam;

a = the azimuth angle of the solar beam (from the south);

a_o = the aximuth angle of a line which is normal to the surface under consideration (from the south);

S = the angle of tilt of the sloping surface (between the surface and horizontal).

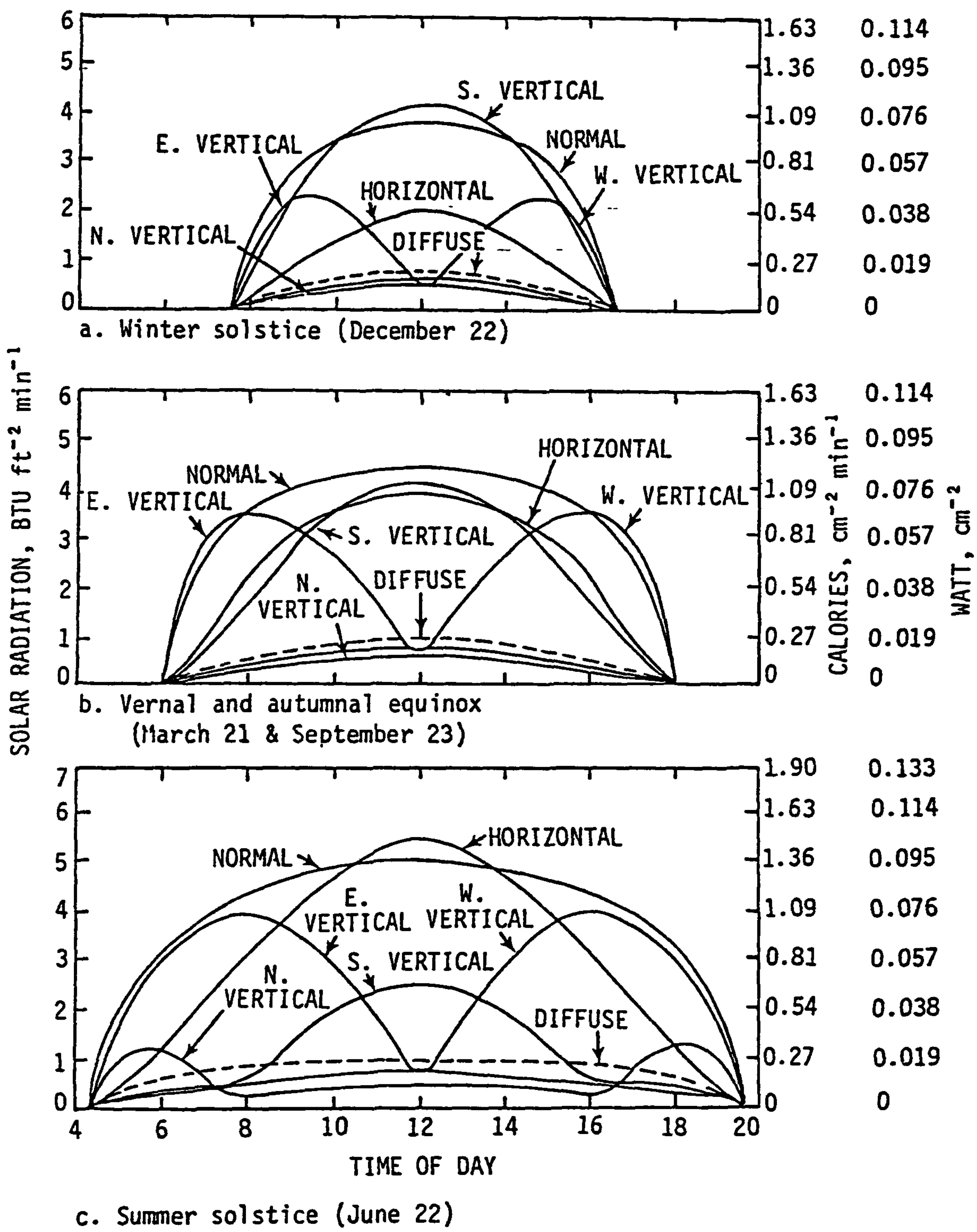
S. VERTICAL
E. VERTICAL
NORMAL
W. VERTICAL
HORIZONTAL
N. VERTICAL
DIFFUSE
a. Winter solstice (December 22)
SOLAR RADIATION, BTU ft^{-2} min^{-1}
CALORIES, cm^{-2} min^{-1}
WATT, cm^{-2}
b. Vernal and autumnal equinox
(March 21 & September 23)
c. Summer solstice (June 22)
TIME OF DAY

Figure 5

Daily or hourly values can be obtained from these instantaneous fluxes by integrating over the period required with respect to changes in Q_0, Z, and a.

Figure 5 provides the variations in incoming direct and diffuse solar radiation for Illinois on clear days at each solstice and equinox. The figures provide plots for a horizontal surface, vertical surfaces facing the four cardinal points of the compass, and for a surface that "tracks" the sun so that the direct beam is always normal to it. The picture obviously becomes much more complex if there is any marked increase in the random component of variability of solar beam attenuation such as caused by clouds. This results in both a net reduction in incoming global radiation, and a change in the ratio of its direct to diffuse components.

The equations of the previous section can be extended by geometric and trigonometric means to provide estimates of the direct and diffuse components of solar radiation on tilted surfaces.

Long-term Trends in Solar Radiation

The only data set which can be used to provide long term trends of global radiation received on a horizontal surface for Illinois is that for Lemont. Table 3 presents monthly means of this data for three periods; namely the whole period of 1950-1978, and two subsections of the whole period, 1950-1964 and 1966-1978. This clearly indicates that there has been a downturn in the annual mean between the two subsections of 7.2%, and also in all monthly means except those for January and February, and with a maximum decrease of 15.0% for September. Figures 6A, 6B and 6C display annual and monthly mean data for each year of record at Lemont from 1950 to 1978 and it is obvious

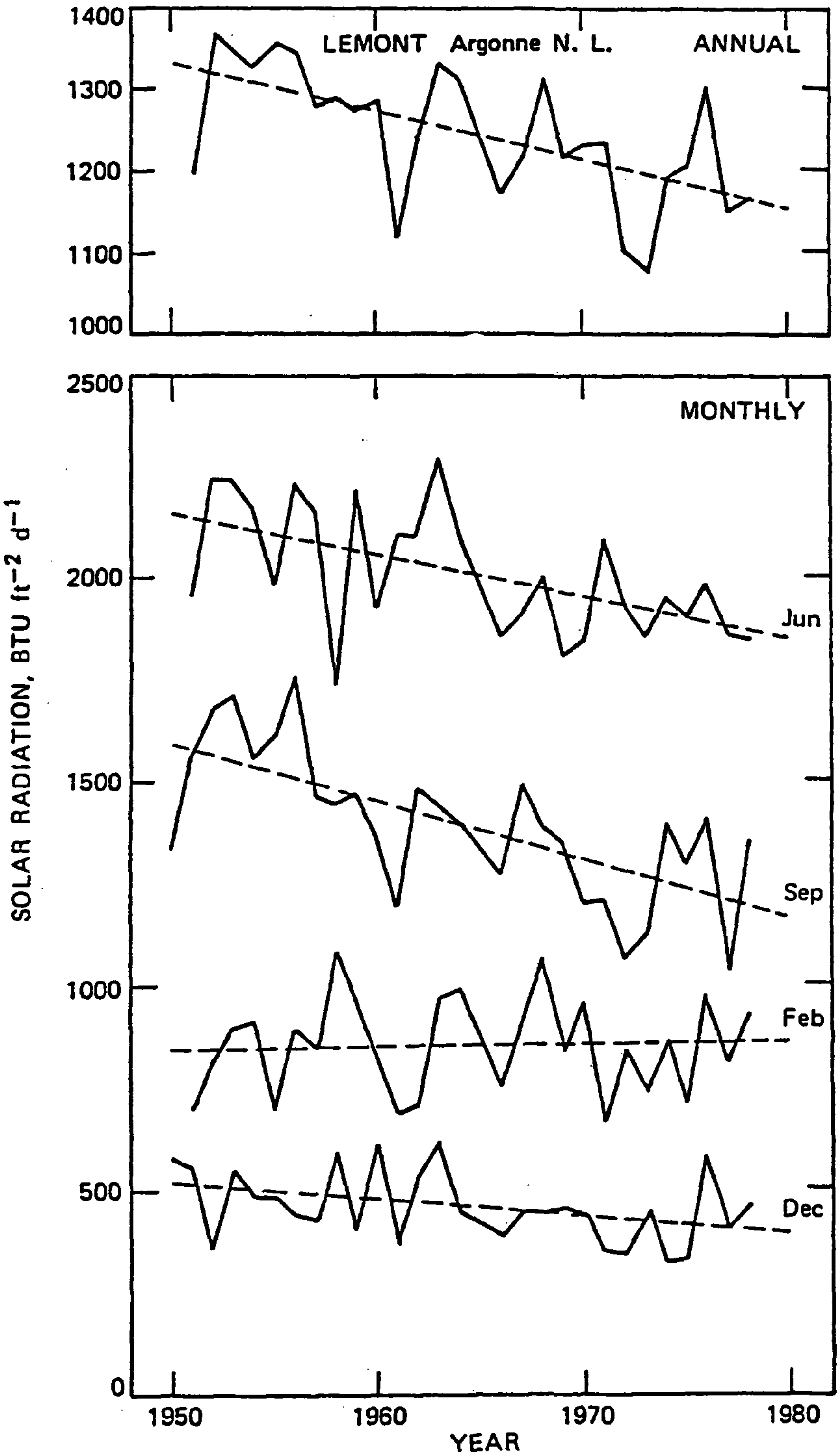
LEMONT Argonne N. L.
ANNUAL
1400
1300
1200
1100
1000
MONTHLY
2500
2000
1500
1000
500
0
Jun
Sep
Feb
Dec
SOLAR RADIATION, BTU ft^{-2} d^{-1}
1950
1960
1970
1980
YEAR

Figure 6A

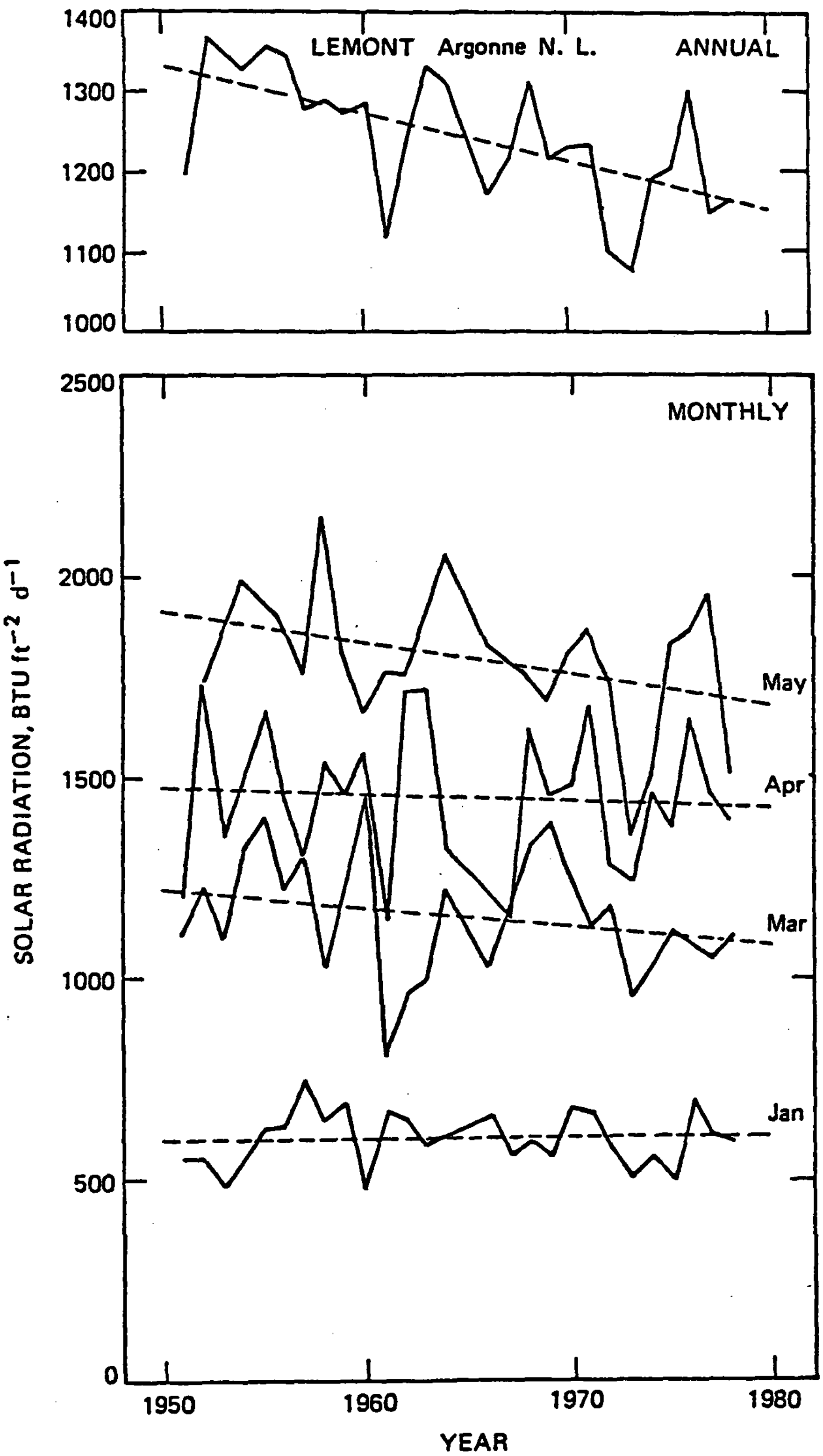
LEMONT Argonne N. L.
ANNUAL
MONTHLY
May
Apr
Mar
Jan
SOLAR RADIATION, BTU ft^{-2} d^{-1}
YEAR
1400
1300
1200
1100
1000
2500
2000
1500
1000
500
0
1950
1960
1970
1980

Figure 6B

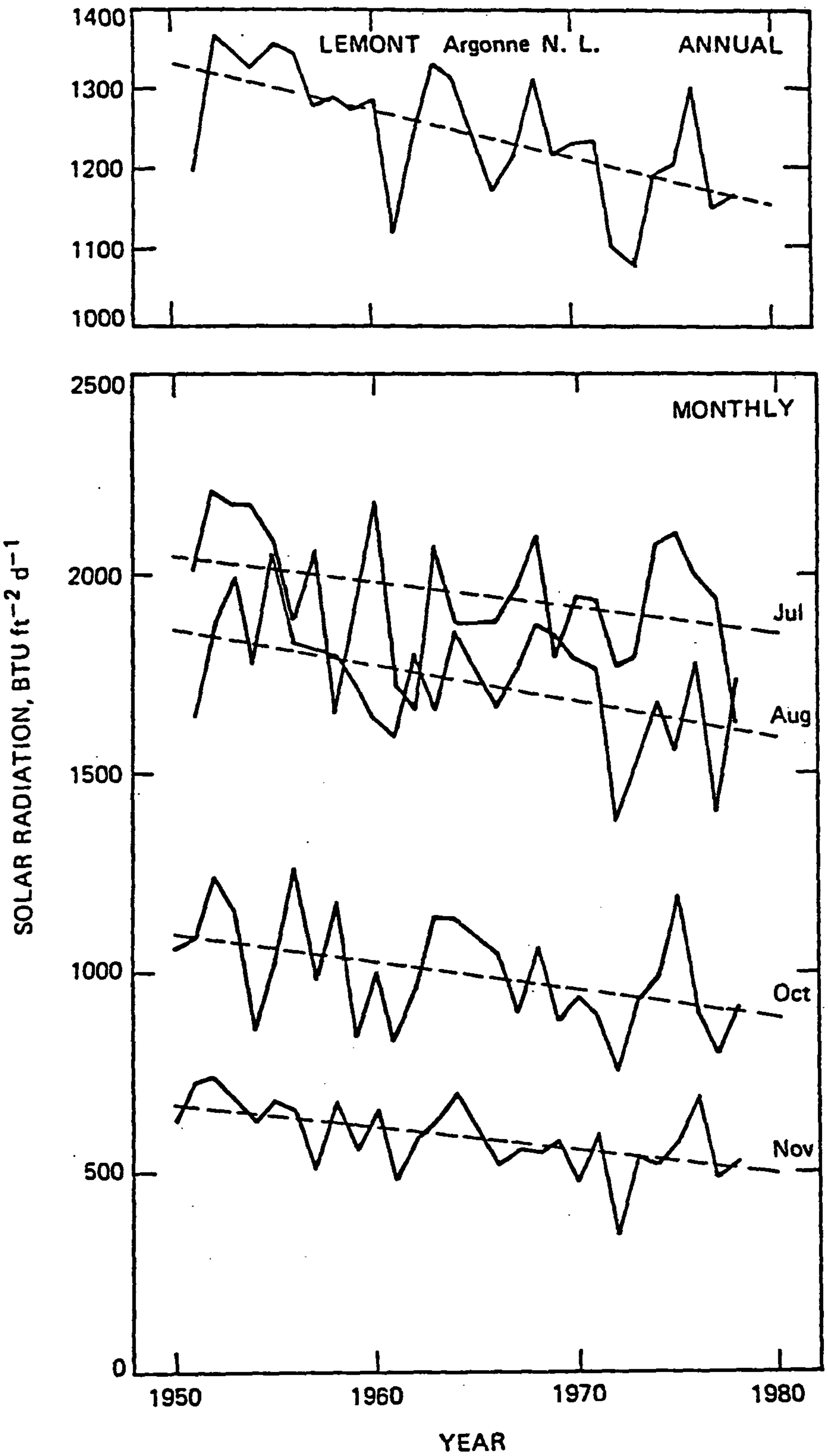
LEMONT Argonne N. L.
ANNUAL
1400
1300
1200
1100
1000
MONTHLY
2500
2000
1500
1000
500
0
Jul
Aug
Oct
Nov
SOLAR RADIATION, BTU ft^{-2} d^{-1}
1950
1960
1970
1980
YEAR

Figure 6C

that for many months, although there is considerable interannual variation, a continued and significant reduction in solar radiation received at the surface is apparent. Lines of best fit were computed for each month and the annual case using a least squares analysis, and coefficients for the regression equation determined. These lines have been plotted for each month using dashes, and are provided separately in Figure 7 on the one set of axes for intercomparison. There has been no change for January or February, and the small decreases evident for both March and April are not statistically significant since they are swamped by the wide scatter in the data. However, in each of the months from May through December, there has been a significant decrease with $r^2 \geq 0.20$ in each case, and having a maximum value of 0.50 for September.

A closer scrutiny of the monthly and annual graphs reveals that for years in which one month is significantly different from the line of best fit, there is a tendency for succeeding months to have the same type of variation. Thus, for annual means that are significant peaks or lows, there tends to be 9 or more of its constituent months that vary in the same way.

This general downward trend for Lemont probably results from the interplay of at least two factors. The urban/industrial effect of the Chicago region as it has expanded towards the Lemont area has resulted in the increase of aerosols in the local atmosphere, thereby reducing its transparency to the solar beam, and also leading to an increase in cloudiness and precipitation. The increase in contrails over the same period has resulted in an increase in cirrus cloud and hence greater reflection of the solar beam before it reaches the surface. Shifting weather patterns leading to changes in the patterns of cloudiness and atmospheric water vapor, and possibilities of undetected calibration drift in the instrumentation may also be contributing factors.

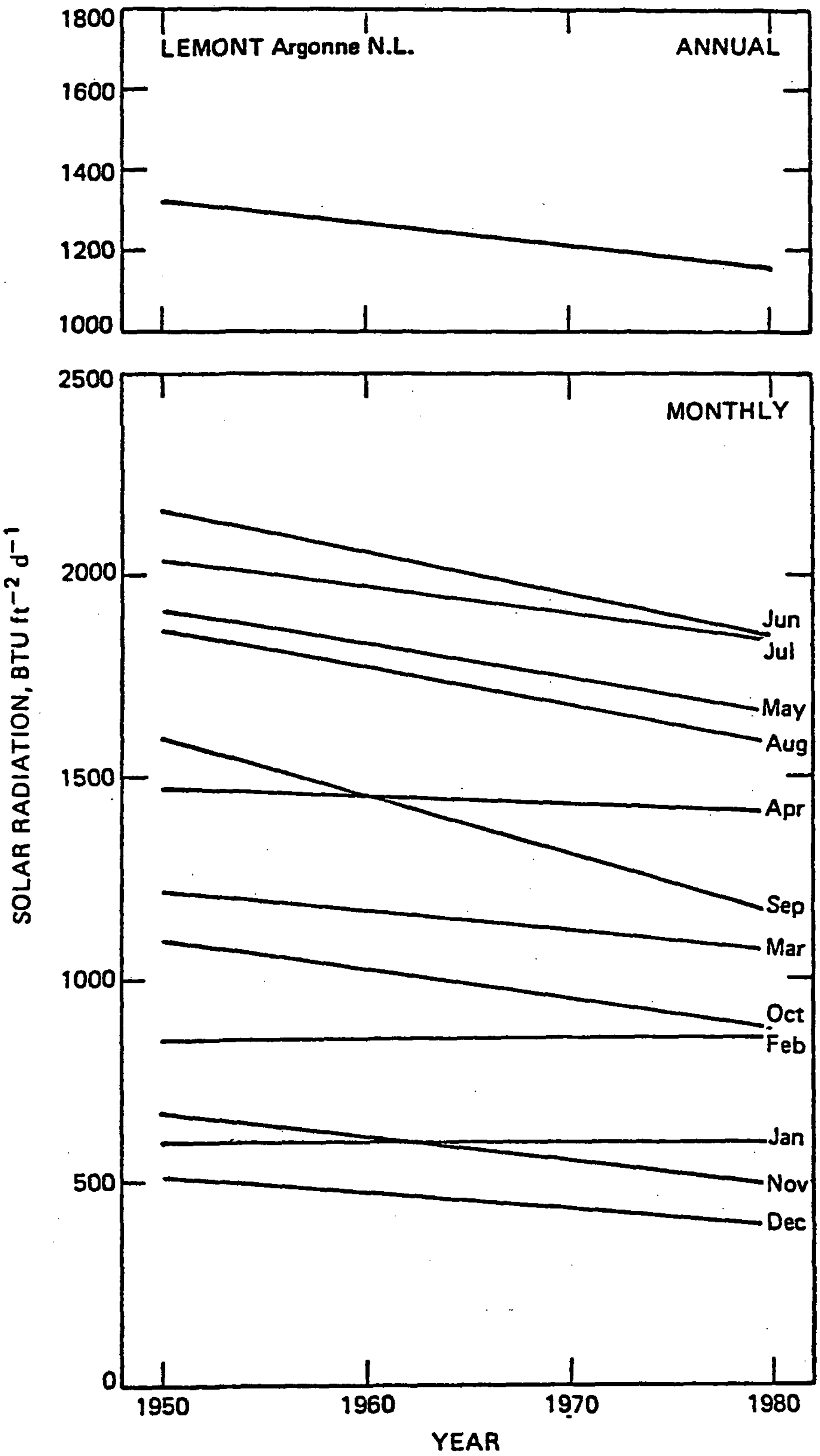
LEMONT Argonne N.L.
ANNUAL
MONTHLY
SOLAR RADIATION, BTU ft^{-2} d^{-1}
YEAR
1800
1600
1400
1200
1000
2500
2000
1500
1000
500
0
1950
1960
1970
1980
Jun
Jul
May
Aug
Apr
Sep
Mar
Oct
Feb
Jan
Nov
Dec

Figure 7

A review of available data for Columbia, MO and Indianapolis, IN revealed similar trends in the case of Indianapolis, but no significant changes for Columbia.

Thus if solar technology is to be implemented as a major strategy, it is imperative that we investigate these urban/industrial effects and long-term changes in incoming solar radiation in more detail. This is very important in the case of Illinois since such a large proportion of its population lives in an urbanized environment that may be subject to such reductions in incoming solar energy, thus making it potentially less cost-effective, or requiring different technology to achieve the necessary energy goals.

References

Knapp, C. L., T. L. Stoffel, and S. D. Whitaker, 1980: Insolation Data Manual. Long-term Monthly Averages of Solar Radiation, Degree Days and Global $\overline{K_T}$ for 248 National Weather Service Stations. Solar Energy Research Institute, Golden, CO, SERI/SP-755-789, 282 pp.

Stoffel, T. L., 1980: Global $\overline{K_T}$ methodology. In Knapp, C. L., T. L. Stoffel and. S. D. Whitaker, Insolation Data Manual, SERI/SP-755-789, Appendix A, 252-253.

Seller, W. D., 1965: Physical Climatology. University of Chicago Press, Chicago, 272 pp.

PROBABILITY OF CONSECUTIVE CLOUDY DAYS

Consecutive days with daytime cloud cover are important when studying the feasibility of solar power, since consecutive cloudy days either require some storage mechanism, or a stand-by, reliable energy source which can be used when solar is inadequate to meet demand. For the purpose of this study, cloudy days were defined as those when cloud cover during the 12 hours between 0600 and 1800 was equal to or greater than 0.8. Analyses were made for Chicago, Springfield and Evansville.

Table 5 shows the average number of cloudy days per month (not necessarily consecutive days) at three stations within or near Illinois for the period 1970-79. Note that the data of the three stations follow a similar annual march, with maximum cloudy frequencies occurring during the winter half-year (18 to 20 days per month), and the minimum frequency occurring during July (9 to 10 days per month).

Tables 6, 7, and 8 present mean monthly frequencies of consecutive cloudy days of various lengths for the three cities analyzed.

The winter half-year is clearly that season with the greatest number of consecutive days with cloud cover (as much as one episode with 20 consecutive cloudy days in Chicago during one November), and winter also exhibits higher frequencies of all numbers of consecutive cloudy days than that observed during any other season. The data presented in Tables 6, 7, and 8 indicate that November and December typically experience the largest numbers of consecutive cloudy days, and July typically experiences minimum frequencies. Winter should be expected to yield the greatest amount of consecutive cloudy days since winter clouds are primarily the result of large scale cloud shields associated with cyclones and fronts, whereas summer clouds are largely composed of convective clouds with relatively small areal extent.

The data of Tables 6, 7, and 8 may be used to estimate the mean number of times per year when given numbers of consecutive cloudy days should be expected based on climatic probabilities. For example, three consecutive cloudy days are expected twice per month from November to May. Five to six consecutive cloudy days are expected once per month during the same period. On the longer time scale, ten consecutive cloudy days are expected only once in 10 years from January through March' whereas 15-20 consecutive cloudy days are expected with the frequency of once in 10 years only during November and December. Probabilities of other frequencies can be obtained from the information presented in Tables 6, 7, and 8.

One should note that the cloud cover information presented for each of the three sites is very much like that of the others, suggesting that all/ much of Illinois experiences much the same probabilities of consecutive cloudy days during the various months of the year.

Table 5. Mean number of cloudy days per month during 1970-79 at three Illinois or near-Illinois sites.

	Jan	Feb	Mar	Apr	May	Jun	Jul	Aug	Sep	Oct	Nov	Dec
Chicago	17.4	17.9	18.7	14.6	13.2	11.7	8.7	11.4	12.4	13.0	17.5	19.4
Springfield	17.0	14.9	19.7	15.0	13.7	11.0	10.4	12.4	11.2	13.0	17.1	18.1
Evansville	18.5	16.0	17.0	14.7	12.8	10.7	9.8	9.8	10.2	11.9	16.0	17.8

Table 6. Number of consecutive cloudy days (2.80% mean daytime cloud cover) at Chicago occurring in 10 year period, 1970-79.

	Consecutive Days With Clouds											
Month	3	4	5	6	7	8	9	10	11	12	13	20
January	22	13	10	6	5	2	2	1				
February	23	12	7	5	3							
March	28	21	13	8	3	2	1					
April	22	10	5	3	2	1	1					
May	19	13	5	2	1							
June	13	5	3	2								
July	10	4	2									
August	13	8	4	2	2	1	1					
September	12	4	3	2	2	1	1	1	1	1		
October	16	11	6	3	1							
November	23	13	9	5	3	2	1	1	1	1	1	1
December	24	14	10	9	8	6	3	1	1	1	1	

Table 7. Number of consecutive cloudy days (≥80% mean daytime cloud cover) at Springfield occurring in 10 year period, 1970-79.

	Consecutive Days With Clouds											
Month	3	4	5	6	7	8	9	10	11	12	15	16
January	24	16	12	8	3	1	1	1				
February	16	9	7	5	1	1	1					
March	29	21	14	7	4	2	2	2				
April	19	13	7	5	3	1	1					
May	20	15	11	5	1							
June	14	8	5	3	1	1						
July	8	5	1									
August	13	9	4	4	2	2						
September	13	8	7	5	5	3	1					
October	18	11	3	1								
November	22	14	10	8	5	3	3	3	2	2	2	1
December	23	14	10	7	5	4	3	3	3	2	1	

Table 8. Number of consecutive days (≥80% mean daytime cloud cover) at Evansville, IN occurring in 10 year period, 1970-79.

	Consecutive Days With Clouds													
Month	3	4	5	6	7	8	9	10	11	12	13	14	15	16
January	28	19	9	4	3	1								
February	21	11	10	7	4	3	1	1	1					
March	21	11	8	5	3	3	3	3	3	2	2	2	1	1
April	22	10	7	4	4	2	1	1	1	1	1			
May	21	12	6	5	1	1	1							
June	12	5	4	2	2	1								
July	11	4	3	2										
August	13	10	8	3	3	1	1	1						
September	9	6	3	1	1									
October	13	7	4	2										
November	23	15	11	7	7	6	1	1	1					
December	25	15	9	9	8	7	6	4	3	2	1			

MEAN MONTHLY TEMPERATURES OVER ILLINOIS

The temperature at any given location and time depends upon the incident solar radiation, the clarity of the atmosphere, concentration of water vapor in the atmosphere, the amount of cloud cover, the reflectivity (albedo) of the surface, the availability of water to be used for evaporation, the strength of advection, topography and several other but lesser significant features. Since temperature is most strongly related to the flux density of incident solar radiation, we find that mean monthly temperatures are greatest in the southern part of Illinois and exhibit lower values as one proceeds northward (see Figs. 8 and 9). The range of values over Illinois in any one month is greatest during the winter season and least during the summer, being about 16°F in January and February and only about 8°F in July and August. Northern Illinois experiences about a 52°F change from mean January temperatures to mean July temperatures, whereas southern Illinois experiences about 44°F change during the same time interval.

The isotherms (lines of constant temperature) almost always exhibit near east-west orientation with two notable areas of deviation from that rule: (1) within central Illinois the isotherms often exhibit a northward bulge, i.e., warmer temperatures than either east or west; and (2) the thermal effect of the Chicago metropolitan area is clearly apparent on these charts. The mean monthly isotherms always indicate the Chicago metropolitan area to be warmer than the area immediately to the west. The effect of Lake Michigan is to warm the Chicago area during winter, and cool the shoreline region during summer. This summer cooling effect is not very apparent on the maps because its extent inland is insufficient to be illustrated at this scale.

MEAN MONTHLY TEMPERATURE (°F)

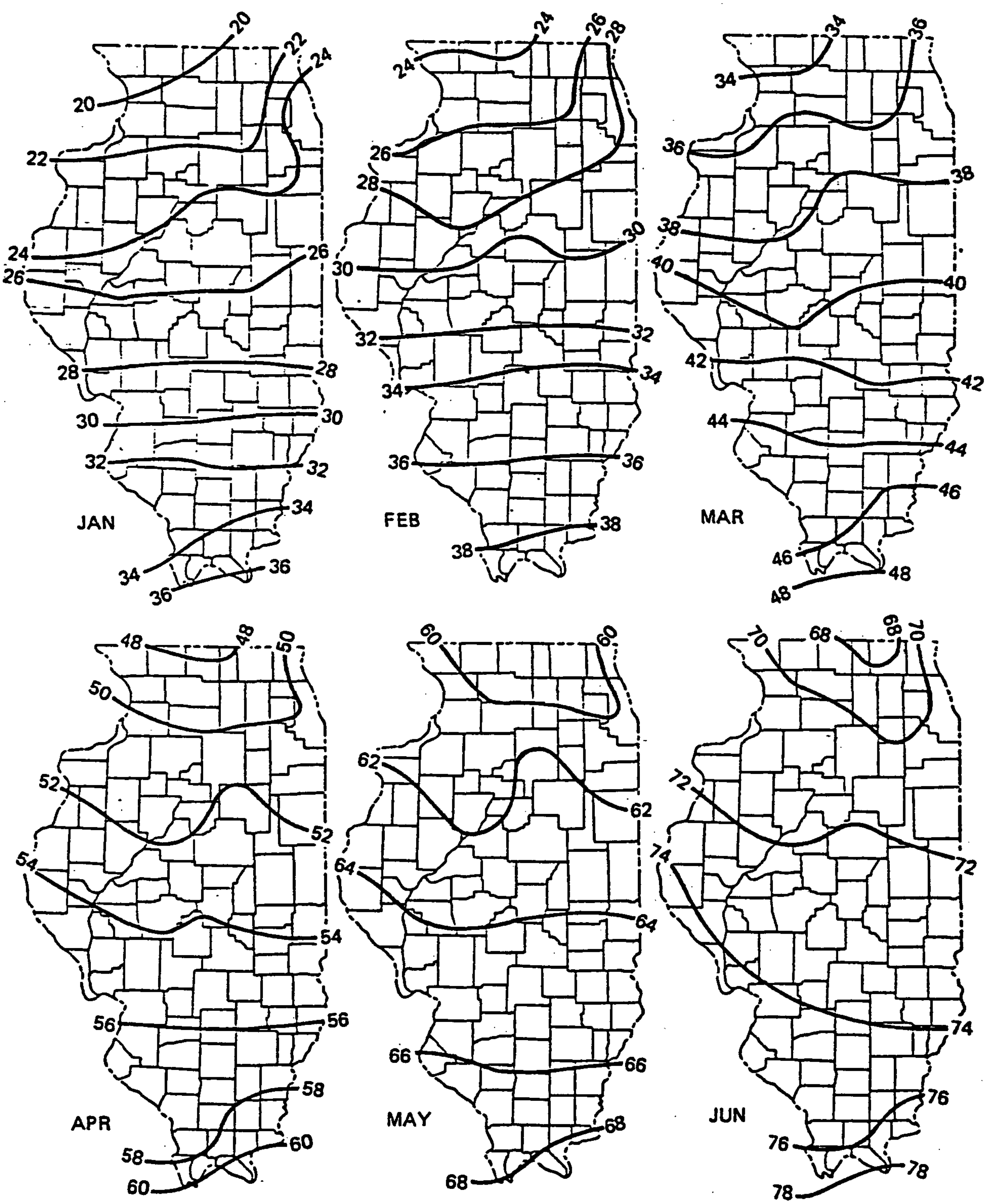

Figure 8

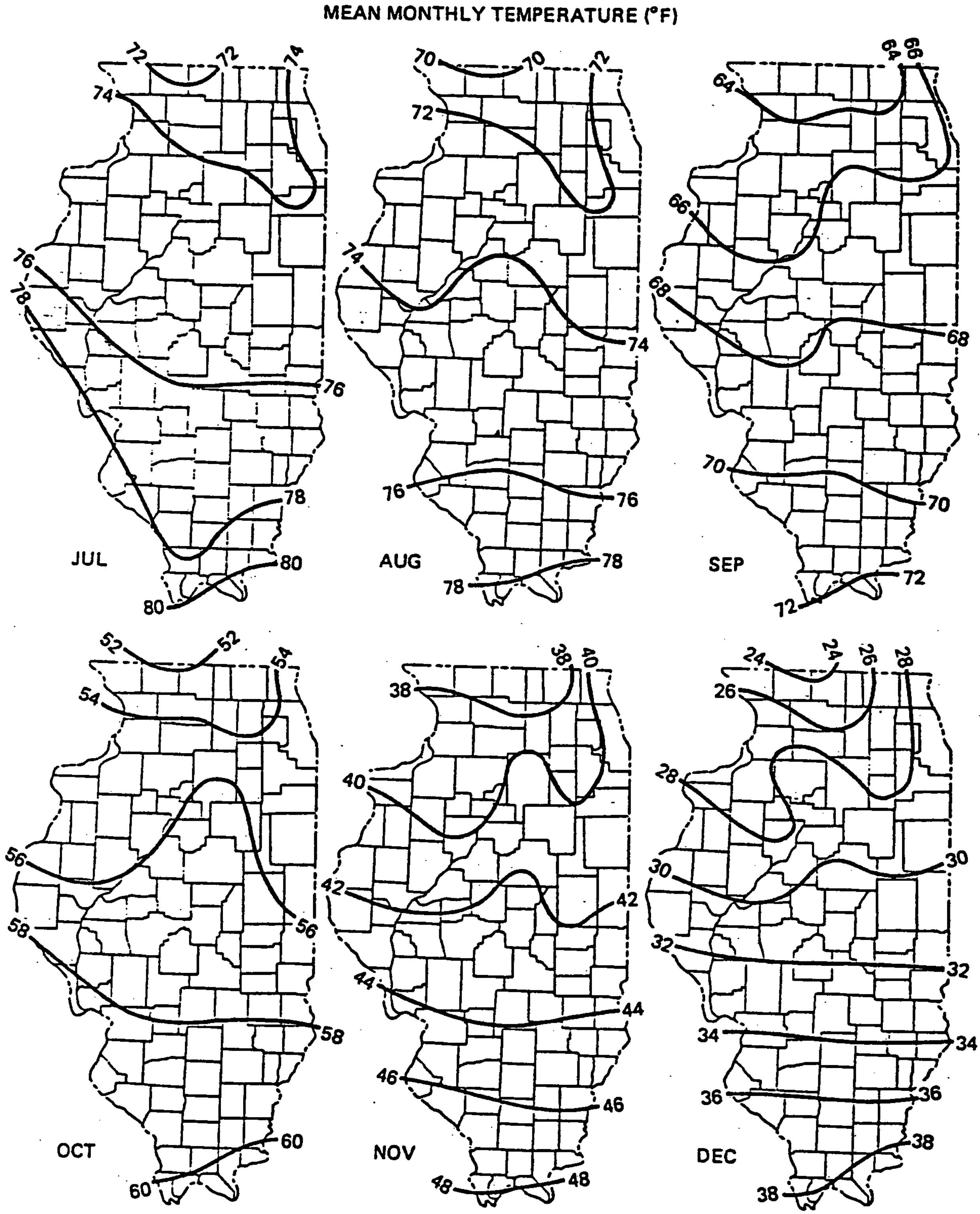
MEAN MONTHLY TEMPERATURE (°F)
JUL
72
72
74
74
76
76
78
78
80
80
AUG
70
70
72
72
74
74
76
76
78
78
SEP
64
64
66
66
68
68
70
70
72
72
OCT
52
52
54
54
56
56
58
58
60
60
NOV
38
38
40
40
42
42
44
44
46
46
48
48
DEC
24
24
26
26
28
28
30
30
32
32
34
34
36
36
38
38

Figure 9

The coldest mean monthly temperatures are always located in the north central and/or the northwestern portion of Illinois.

The mean annual diurnal (daily maximum temperature minus the minimum temperature) is about 20°F throughout Illinois, being slightly diminished during the winter season and slightly enhanced during summer. Specifically, the mean diurnal temperature variation over Illinois is about 16°F in January and about 20°F during July. There is no clear or systematic spatial distribution of diurnal temperature ranges over Illinois during any season.

Mean daily maximum temperatures may be obtained by adding 8°F to the mean daily temperatures given in Figures 8 and 9 during the winter season or by adding 10°F to the mean daily temperature shown for summer. Similarly mean daily minimum temperatures in winter may be found by subtracting 8°F from the mean daily temperature and subtracting 10°F from mean daily temperatures during summer.

Summer extreme (record) temperatures vary from about 105°F in northern Illinois to about 110°F in the south. Winter extremes in the north are about -25°F to -10°F in the south.

DEGREE DAYS

Degree days are a "surrogate" weather parameter (i.e., a parameter not directly measured in the environment, but one which is calculated, based on certain assumptions). Heating degree days are a measure of the amount of energy required to bring a building up to the comfort level when the temperature is relatively cold outside. The comfort level is assumed to be 65°F (19°C), and daily heating degree days are obtained by subtracting the mean daily temperature from 65. These daily differences are accumulated as heating degree days for the entire heating season beginning in July of each year and ending on 30 June of the following year. The range of annual heating degree days over Illinois for an average year varies from about 4000 at Cairo to about 7000 along the Wisconsin-Illinois border.

Cooling degree days, on the other hand, are calculated by subtracting 65°F from the daily mean temperature and accumulating the daily differences during the cooling season which begins 1 January and concludes 31 December of each year. Annual cooling degree days totals are much smaller than annual heating degree days in Illinois, varying from 1700 cooling degree days at Cairo to about 600 cooling degree days in northern Illinois.

Heating Degree Days

The mean monthly heating degree days are shown for each month of the year in Figures 10 and 11. The totals for June, July, and August are in all cases less than 50 heating degree days per month in Illinois. As one would expect, the greatest number of heating degree days is found in the northern part of the state with the least amount exhibited over the southern counties.

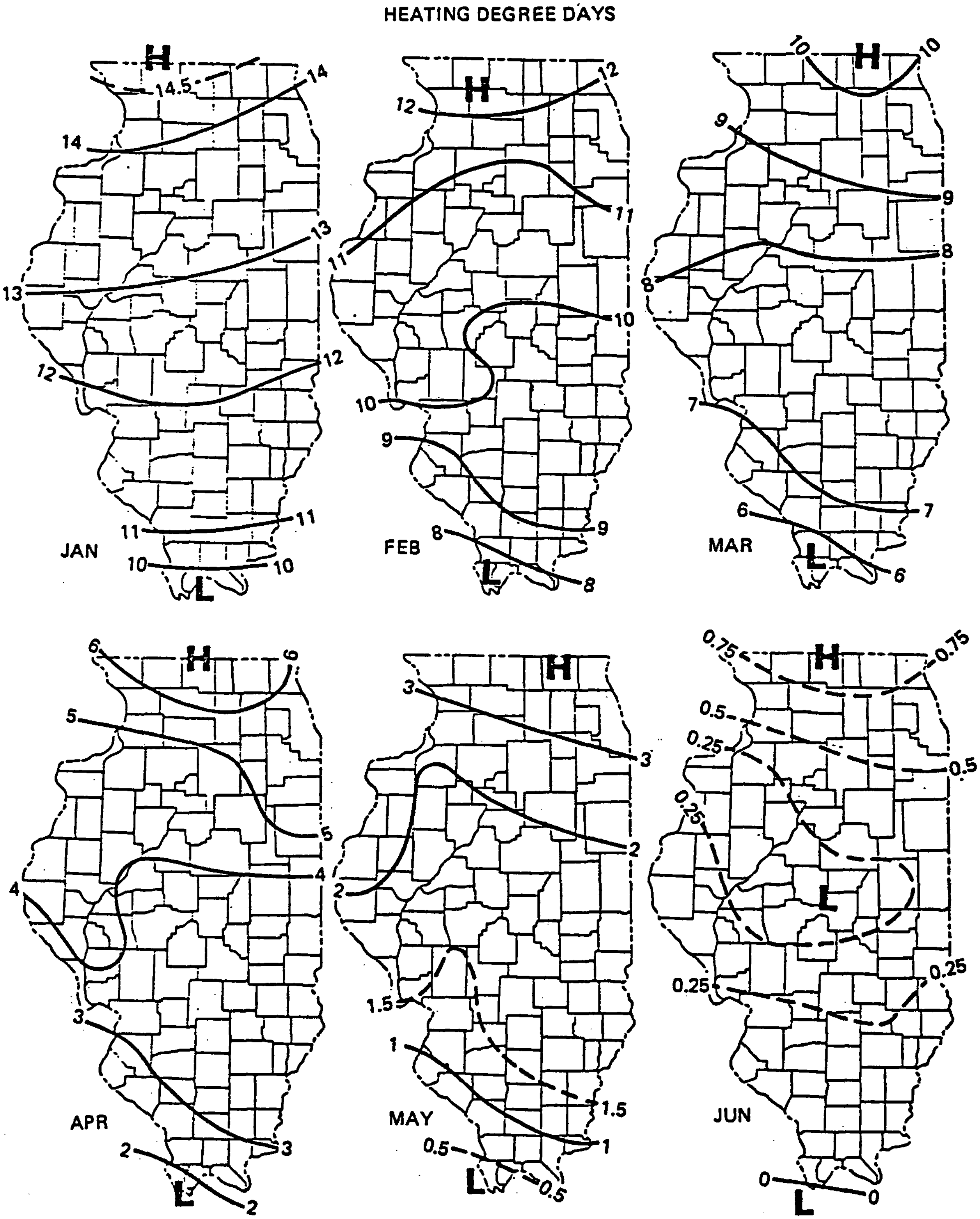
HEATING DEGREE DAYS
JAN
FEB
MAR
APR
MAY
JUN
H
L
14.5
14
13
12
11
10
9
8
7
6
5
4
3
2
1.5
1
0.75
0.5
0.25
0

Figure 10

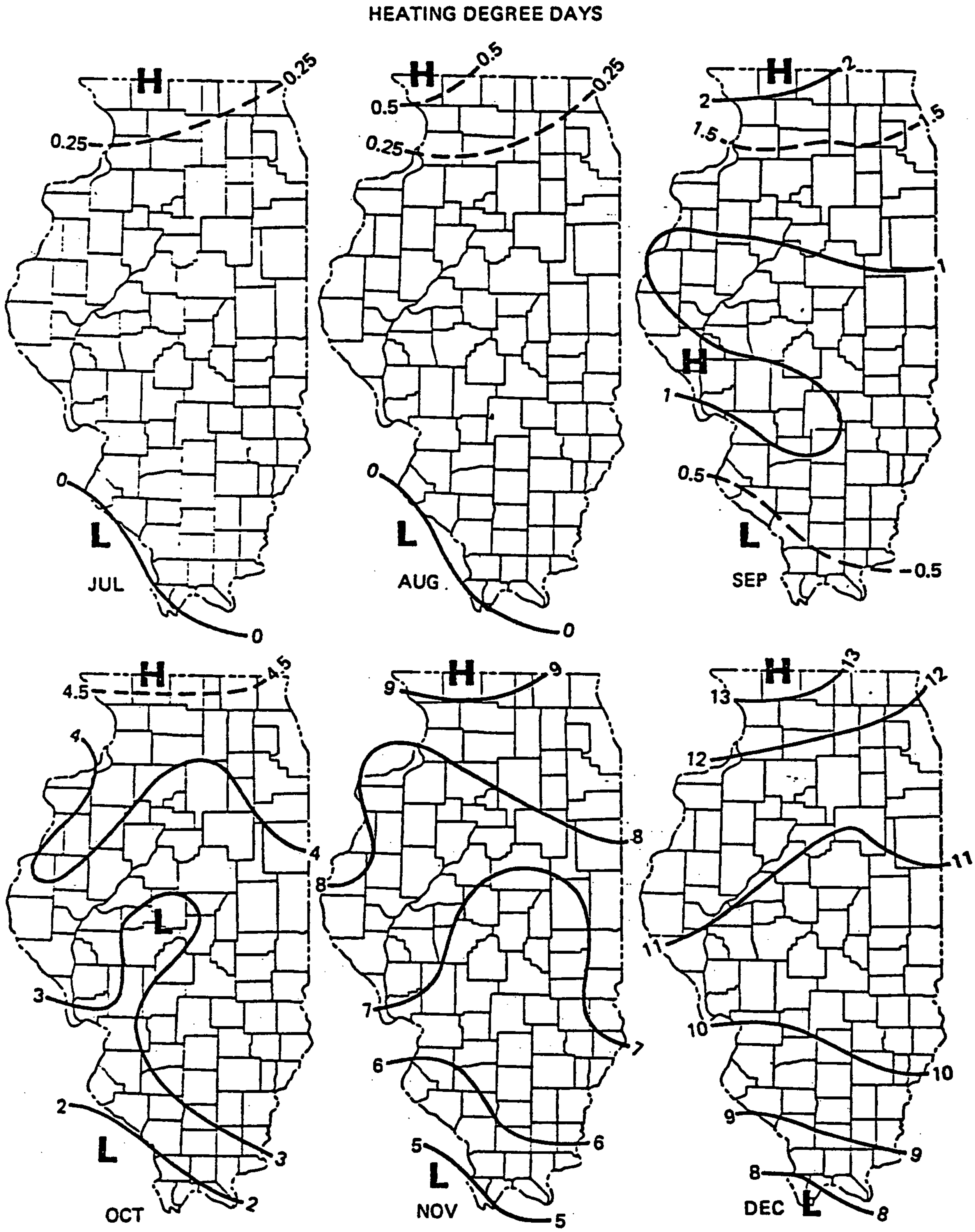
HEATING DEGREE DAYS
H
0.25
0.25
0
L
JUL
0
H
0.5
0.5
0.25
0.25
0
L
AUG
0
H
2
2
1.5
1.5
1
H
1
0.5
L
SEP
0.5
H
4.5
4.5
4
4
L
3
2
L
3
OCT
2
H
9
9
8
8
7
7
6
6
5
L
NOV
5
H
13
13
12
12
11
11
10
10
9
9
8
DEC
L
8

Figure 11

During each of the months with greatest heating degree days (November through April) the gradient of heating degree days is strongly oriented north to south, i.e., the totals regularly decrease toward the south. During the remaining months, the contours of equal heating degree days are rather convuluted with the central part of the state (the area around Sangamon County) being relatively less than west, north, or east.

Cooling Degree Days

Although the greatest accumulation of cooling degree days is always found in the southern part of the state (see Fig. 12) and the smallest totals in the northern part of the state, the patterns are complex with the central part of the state (roughly including Sangamon, Logan, Macon, DeWitt, and Piatt Counties) being relatively higher than either west, north, or east.

The influence of the Chicago metropolitan area is apparent on the cooling degree day distribution of all months shown. A large metropolitan area is almost always warmer than the surrounding area because of the thermal characteristics of the building materials used in a city as well as the large number of sources of heat generated for space heating. In all months shown, but particularly July and September, the Chicago area experiences more cooling degree days than the areas immediately surrounding it. This is true in spite of Lake Michigan acting as a cooling source, since it only affects its immediate periphery.

COOLING DEGREE DAYS

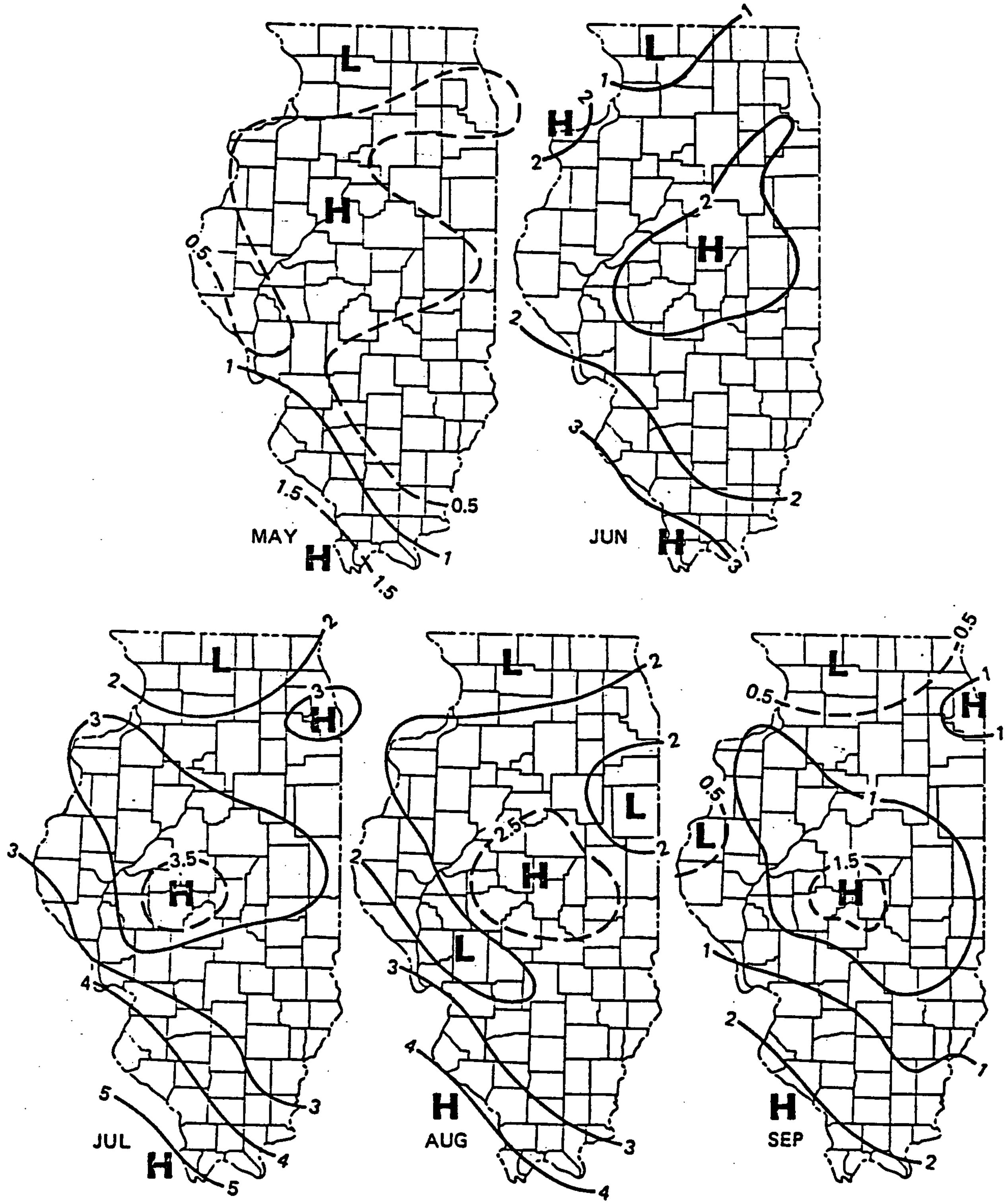

Figure 12

ANNUAL MARCH OF RELATIVE HUMIDITY OVER ILLINOIS

Warm air is able to contain more water vapor than cold air. For example, air with a temperature of 75°F can hold about 4 times more moisture than air with a temperature of 40°F. Typical air on a summer day in Illinois with the temperature of 86°F can contain almost thirty times more water vapor than air at only 14°F on a winter day. Air is saturated, i.e., contains all the water vapor that the air *can* contain at that temperature, on few occasions; those being times of fog and heavy rainfall. On most days of the year, the air contains less than 100% of its maximum potential water vapor.

The *relative humidity,* while being simple to obtain by measurement, is a rather complex quantity. At any time, the atmosphere contains some quantity of water in the form of vapor, and there is thus a (partial) pressure generated by the molecular motion of this water vapor, referred to as the actual vapor pressure of the atmosphere. Additionally, for any given temperature and pressure, the atmosphere has a maximum potential capacity for water vapor, and the pressure which it would generate, if present, is called the saturation vapor pressure of the air at that temperature and pressure. The relative humidity of the air at any given temperature and pressure is the ratio of the actual vapor pressure to the saturation vapor pressure and is usually expressed as a percentage. The theoretical limits to relative humidity are 0% (although never observed in practice) and 100% (although in odd cases of supersaturation it may exceed 100%). In practice, the lowest relative humidities are observed at the peak of daytime heating over expansive desert areas or over high Arctic/Antarctic areas, when it may reach values as low as 5%. Conversely, values around 100% are achieved with fog, drizzle or heavy rainshowers. Typical low values of relative humidity for Illinois are about 25%.

Because the absolute amount of water vapor in the air tends to be constant from one time of the day to another, and because warm air can potentially hold more water vapor than cold air, and because temperature is typically greater during the daytime than during the night, relative humidity tends to follow a similar trend during a day, regardless of month or season. In general, relative humidities tend to be less during daytime than during nighttime. More specifically, the maximum relative humidity during a day is typically reached shortly after sunrise at the time of minimum temperature, and the minimum relative humidity is usually reached at the time of maximum daily temperature during the middle or late afternoon.

Figures 13 and 14 show the mean relative humidities for 6 a.m. and 6 p.m. for January, April, July, and October for select stations in Illinois. First, one should note that whereas the 6 a.m. relative humidities are generally between 75% and 85%, those of 6 p.m. are typically between 55% and 70%. The 6 a.m. relative humidity values tend to be high (80% or more) over most of the state, largely a result of this being about the time of minimum temperature, and hence the time of minimum saturation vapor pressure, This in turn means that the ratio of actual to saturated vapor pressure is going to be at its highest. The 6 p.m. values tend to reflect the diurnal heating effect leading to higher saturation vapor pressure (and lower relative humidities) in combination with effects of moisture advected into the region by the prevailing air mass, and the more local effects of the Great Lakes.

The distribution of average relative humidities over Illinois does not exhibit great continuity from month to month, except that the highest relative humidities at 6 a.m. tend to be found in the central area of the state. At 6 p.m. there is a slight tendency for the southern part of the state to experience slightly less relative humidity than in the north.

Average relative humidity values for the intervening months are very similar to those values presented here, though the patterns and gradients may be quite different.

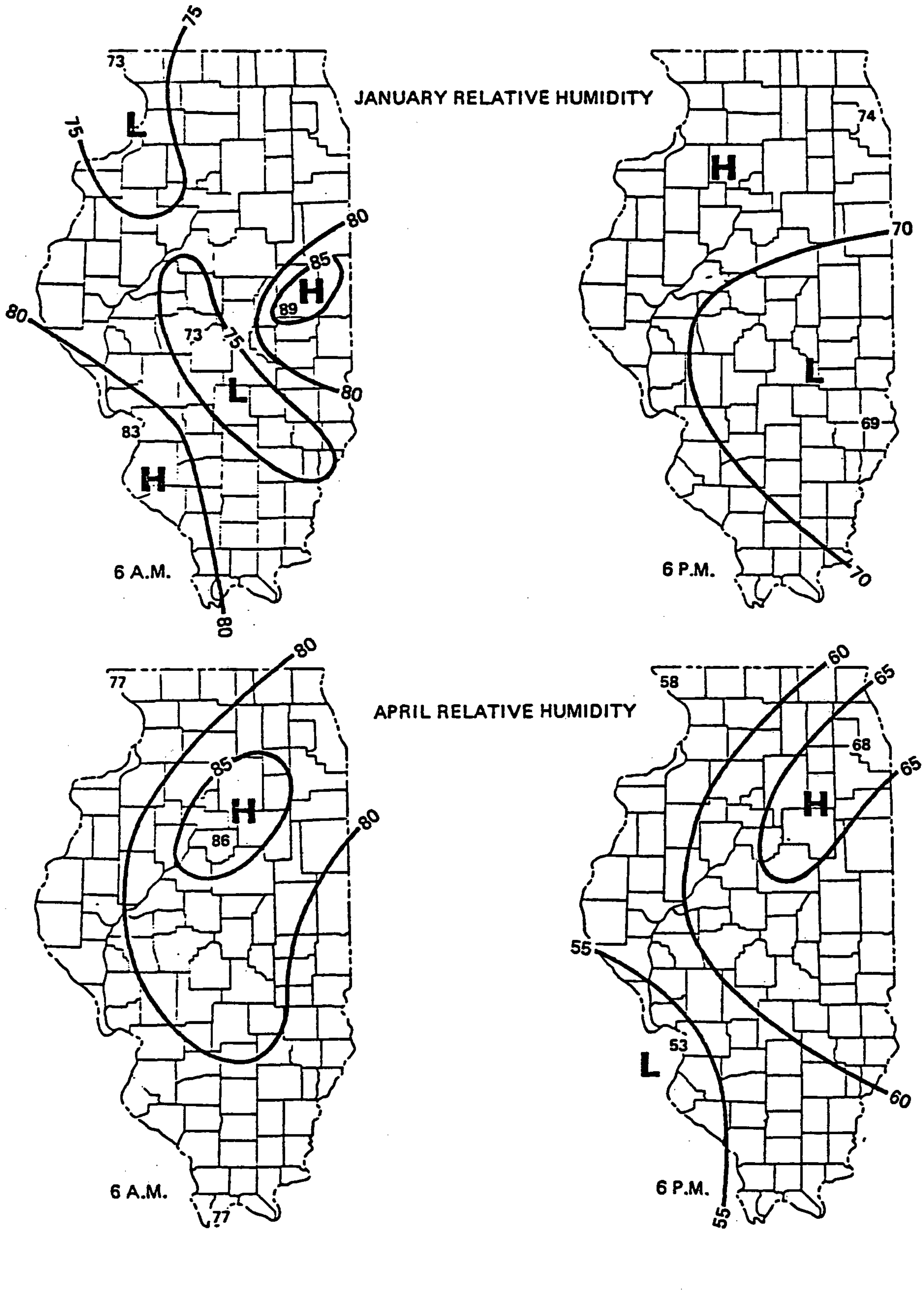
JANUARY RELATIVE HUMIDITY
6 A.M.
6 P.M.
APRIL RELATIVE HUMIDITY
6 A.M.
6 P.M.

Figure 13

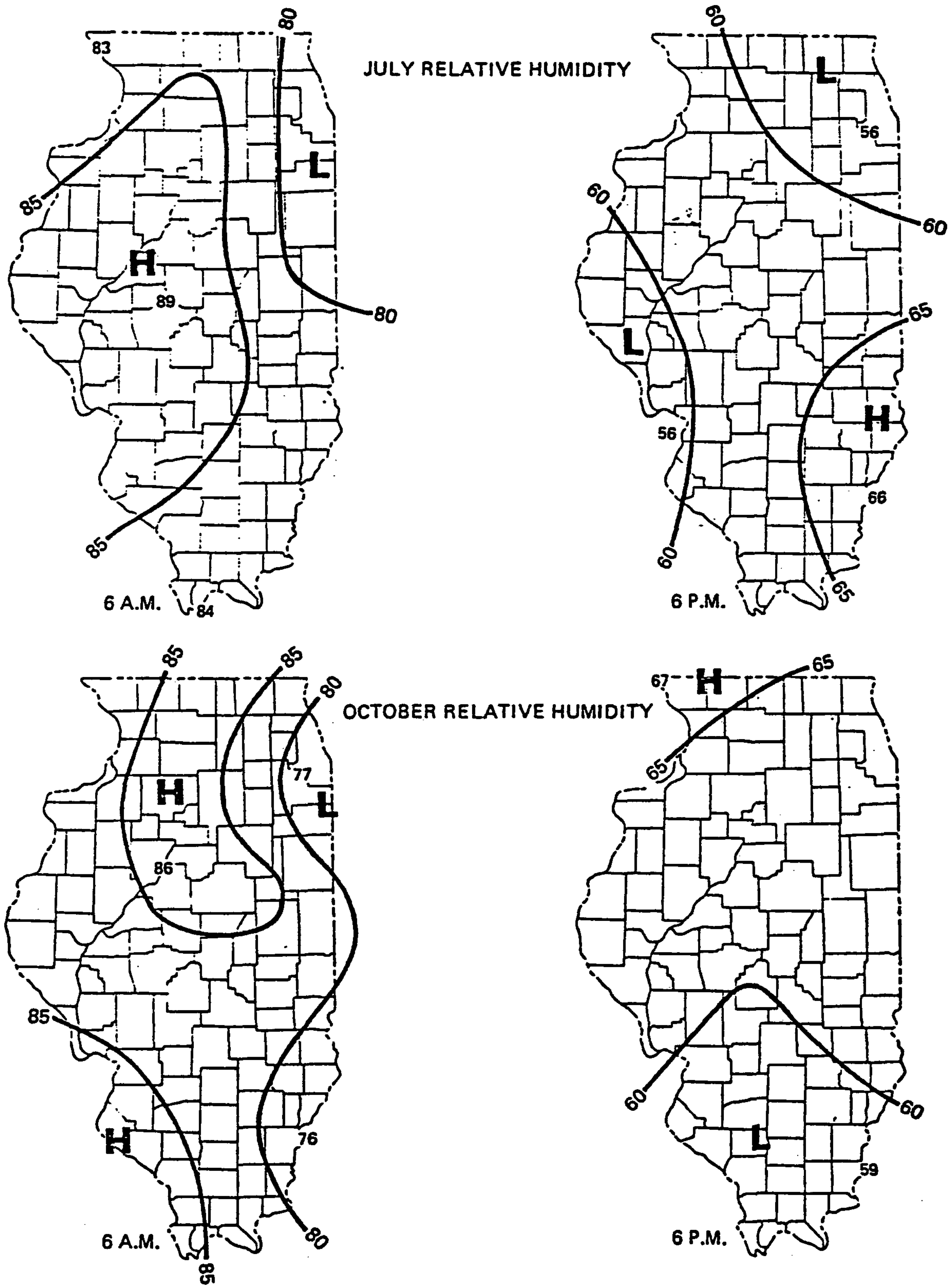
JULY RELATIVE HUMIDITY
83
80
85
L
H
89
80
85
6 A.M.
84
60
L
56
60
60
L
65
H
56
66
60
65
6 P.M.
OCTOBER RELATIVE HUMIDITY
85
85
80
H
77
L
86
85
H
76
80
6 A.M.
85
67
H
65
65
60
60
L
59
6 P.M.

Figure 14

ILLINOIS WIND CLIMATOLOGY

Reliable records of wind speed and direction in Illinois are limited to only a few stations, those being the first-order weather stations of the National Weather Service plus the Urbana record.

Table 9 shows the prevailing wind direction and the average wind speed (raph) for all months of the year for the eight stations included in this study. One will notice that there is little spatial continuity in prevailing wind directions during any one month. This undoubtedly is because small scale surface differences exert an influence on surface winds, e.g., lake-land breeze. Mean monthly wind speeds follow the same general trend through the year at each of the 8 stations, i.e., strongest winds generally being observed from November through about April or May, vrith weaker winds from May or June through October. The average monthly wind speeds are confined to a relatively narrow range, being on the order of from about 5 mph to a maximum of about 13 mph. Slower speeds are recorded in the mean at Cairo, Evansville, and Champaign with the strongest speeds being observed at Chicago, Peoria, and Springfield.

Table 10 shows the "fastest mile" and direction recorded at each of the eight stations for each month of the year. The *fastest mile* is defined as the shortest time during a 24 hour period required for one mile of air to "pass" the anemometer. The length of time is converted to miles per hour. Fastest mile values range from a minimum of 36 mph at Cairo in September, to a maximum of 75 mph at Peoria during July. It is interesting to note that although the sustained average wind speeds tend to be greatest during winter and early

Table 9. Mean monthly wind speed (mph) and prevailing direction.

	Jan	Feb	Mar	Apr	May	Jun	Jul	Aug	Sep	Oct	Nov	Dec
Cairo	(SW) 9.8	(NE) 9.8	(SW) 10.6	(SW) 10.2	(SW) 8.2	(SW) 7.4	(SW) 6.5	(NE) 6.2	(NE) 7.0	(S) 7.3	(S) 9.1	(S) 9.3
Chicago	(W) 11.5	(W) 11.5	.(H) 11.9	(W) 11.8	(SSW) 10.4	(SW) 9.5	(SW) 8.4	(SW) 8.2	(S) 9.0	(S) 9.9	(SSW) 11.3	(W) 11.2
Evansvllle	(SSW) 9.4	(NW) 9.7	(WNW) 10.4	(SSW) 9.9	(SSW) 8.1	(SW) 7.3	(SW) 6.3	(SW) 5.9	(SSW) 6.5	(NW) 7.0	(NW) 8.8	(NW) 9.1
Peoria	(S) 11.2	(WNW) 11.5	(WNW) 12.3	(S) 12.2	(S) 10.3	(S) 9.2	(S) 8.0	(S) 7.8	(S) 8.6	(S) 9.5	(S) 11.1	(S) 11.0
Rockford	(WNW) 10.4	(WNW) 10.6	(ESE) 11.6	(WNW) 11.7	(ENE) 10.6	(SSW) 9.3	(SSW) 8.1	(SSW) 7.9	(SSW) 8.6	(SSW) 9.5	(WNW) 10.4	(WNW) 10.4
Springfield	(NW) 12.9	(NW) 12.9	(NW) 14.0	(S) 13.5	(SSW) 11.6	(SSW) 10.0	(SSW) 8.5	(SSW) 8.0	(SSW) 9.1	(S) 10.5	(S) 12.7	(S) 12.8
St. Louis	(NW) 10.4	(NW) 10.8	(WNW) 11.8	(WNW) 11.4	(S) 9.4	(S) 8.7	(S) 7.8	(S) 7.5	(S) 7.9	(S) 8.7	(S) 9.9	(WNW) 10.3
Champaign	(SW) 8.3	(S) 8.3	(S) 8.7	(S) 8.6	(S) 7.1	(SW) 6.1	(SW) 5.0	(SW) 4.9	(SW) 5.3	(SW) 6.3	(S) 7.9	(S) 8.2

Table 10. The monthly fastest mile (mph) of wind of select Illinois stations.

	Jan	Feb	Mar	Apr	May	Jun	Jul	Aug	Sep	Oct	Nov	Dec
Cairo	50(SW)	56(SW)	60(NW)	59(SW)	49(SW)	60(SW)	45(SW)	44(NW)	36(NE)	40(SW)	53(SW)	63(SW)
Chicago	50(W)	51(SW)	54(NW)	50(NW)	54(S)	50(W)	46(NW)	54(NW)	48(SW)	45(. S)	60(SW)	50(SW)
Evansville	47(W)	59(w)	56(S)	54(NW)	55(NW)	58(NW)	53(NW)	49(NW)	49(SW)	37(S)	47(SW)	56(SW)
Peoria	54(S)	52(W)	56(WNW)	66(SW)	61(SW)	66(N)	75(NW)	65(W)	73(W)	60(SW)	56(W)	58(SW)
Rockford	40(W)	45(WSW)	46(WSW)	54(ESE)	47(WSW)	46(NW)	50(WNW)	48(W)	52(SW)	37(WSW)	46(SW)	44(WNW)
Springfield	65(SW)	63(SE)	66(SW)	60(W)	58(W)	75(SW)	73(SW)	58(W)	52(SW)	45(W)	57(S)	66(SW)
St. Louis	41 (W)	46(NW)	45(NE)	45(W)	42(SW)	60(SE)	42(N)	48(NW)	39(SW)	48(SW)	41 (S)	44(W)
Champaign	71 (M)	65(M)	63(M)	60(M)	54(M)	65(M)	61 (M)	66(M)	52(M)	52(M)	70(M)	81 (M)

M = Missing Data

spring, the months exhibiting the fastest mile occur during the summer. There appears to be no systematic trend of the fastest mile statistics through an average year, probably due to the fact that the observational period is still rather short and that gusts are a relatively small areal meteorological feature, are very short term in length of tenure, and are the result of several meteorological conditions which can conceivable occur during any month of the year.

DIURNAL WIND SPEED VARIATION

Air movement (wind) is basically caused by differential heating over adjacent surfaces. Differences in heating result in differences in pressure yielding a pressure gradient force, which is the basic force of air motion. The larger the pressure gradient force (which is dependent upon forces other than only temperature gradients), the greater the wind speed. Because spatial temperature differences are generally enhanced during the daytime due to solar heating, pressure gradients and associated wind speeds tend to be greater during the day than during the night. On the annual scale, wind speeds are typically greatest during the winter season in middle latitudes, again, because the horizontal temperature gradients are stronger at that time than during other seasons.

Figure 15 shows the percent of daytime (0700-1800) and nighttime (1900-0600) hours when the winds over seven stations in Illinois were greater than 10 mph (1978-79). The centerline of both the daytime and the nighttime winds represents the mean, the limit of shading represents plus and minus one standard deviation. Several characteristics become immediately apparent:

1. frequencies of winds greater than 10 mph are highest during late winter and early spring;
2. the frequency of winds greater than 10 mph is greater during the daytime than during the nighttime;
3. the standard deviation of wind variation during the daytime is greatest during late summer and early fall when the absolute frequencies are lowest;

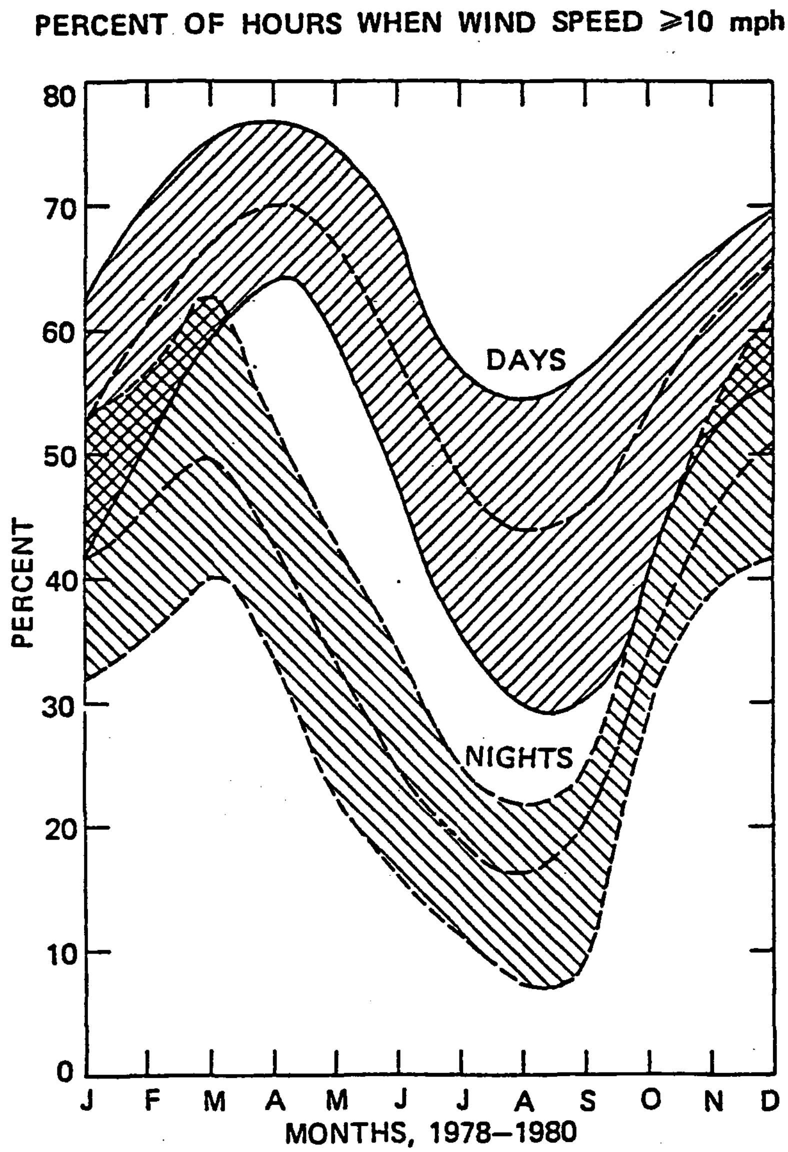
PERCENT OF HOURS WHEN WIND SPEED ≥10 mph
80
70
60
50
40
30
20
10
0
PERCENT
DAYS
NIGHTS
J F M A M J J A S O N D
MONTHS, 1978–1980

Figure 15

4. the standard deviation of the nighttime winds is greatest during late winter-early spring; and

5. nighttime wind frequencies are usually 30-40% of daytime frequencies.

The distribution of monthly mean wind speeds is expected to be very similar to Figure 15. From this information one may safely conclude that the potential for using wind as an alternative energy source is greater during the day than during the night, and greatest during late winter-early spring than any other season of the year in the mean. Winter electrical demand is greatest during the early evening because of the need of lighting, and cooking demands, whereas summer demand is greatest during the day due to air conditioning.

Variation of Wind Speed with Altitude Above the Ground

One of the forces that affects wind speed is friction between the moving air and the ground surface; the greater the friction the slower the pressure induced wind speed. As one ascends in the atmosphere, the impact of surface friction decreases because the rough surface becomes further separated from the air being considered. Since friction decreases with increasing altitude, wind speeds typically are stronger at heights than near the surface of the earth. In addition to friction, the change in wind speed with altitudeis also dependent upon the stability of the air. The wind increases in speed with increasing altitude in almost all cases, however, the rate at which the speed increases varies as a function of both friction and stability.

In the absence of observation of wind speed at several altitudes, a vertical wind profile may be estimated from the observed wind speed at one known height. An equation often employed to calculate winds aloft is of the power form:

$$V_2 = V_1\left(\frac{Z_2}{Z_1}\right)^{\alpha}$$

where V_2 is the estimated wind speed at some altitude (Z_2), V_1 is the measured wind speed at altitude Z_1, and α is an empirically derived power. Since the value of a depends upon the nature of the surface, and hence the friction, and also the atmospheric stability, we suggest daytime values of 0.143 and nighttime values of 0.10 are reasonable estimates for a over central Illinois in the absence of better information.

The Influence of Topography on Wind Speed

Just as wind speeds typically decrease as one comes closer to the surface of the earth due to increased friction, areas of increased friction (rougher surfaces) typically experience slower wind speeds than relatively flat, homogeneous smooth surfaces. Although Illinois may be considered a relatively featureless topographic state, there are some areas with significant differences of relief. For example, the northwestern counties represent the southernmost extension of the "driftless" area where relief is typically on the order of a few hundred feet within a quarter-mile distance. In the southeastern one-third of Illinois, relief is of the same order as that in the northwest. In the area between these two extremes, the surface exhibits only very slight undulations in altitude.

Because of increased topographic relief in the northwestern and southeastern parts of the state, mean wind speeds and the frequency of strong winds are greater along a band that runs roughly from Chicago to St. Louis, with decreasing amounts towards the northwest and southeast. Figure 9 shows a preliminary estimate of the percent of all hours of the year when the winds are greater than 10 mph over Illinois (based on 1978 and 1979 data only). Notice that maximum frequencies are about 52% within the northeast-southwest trending band, with values of about 40% in the northwestern part of Illinois and about 35% in the southeast.

One can see from these observations that the greatest potential for wind power exists in a northeast-southwest trending band from Chicago to St. Louis. That is not to say that there are no other areas in Illinois where the wind speeds are as great as they are on the average within that maximum band. Clearly, there are such regions, like the lakeshore of Lake Michigan, hilltops, and other open exposed areas, where the wind speeds will be greater than what they are at the airport sites in the band of maximum potential. It is appropriate to say, however, that at this scale of analysis, one would expect to find more suitable areas for the generation of electric power in the band from Chicago to St. Louis than in other sections per unit area of the state.

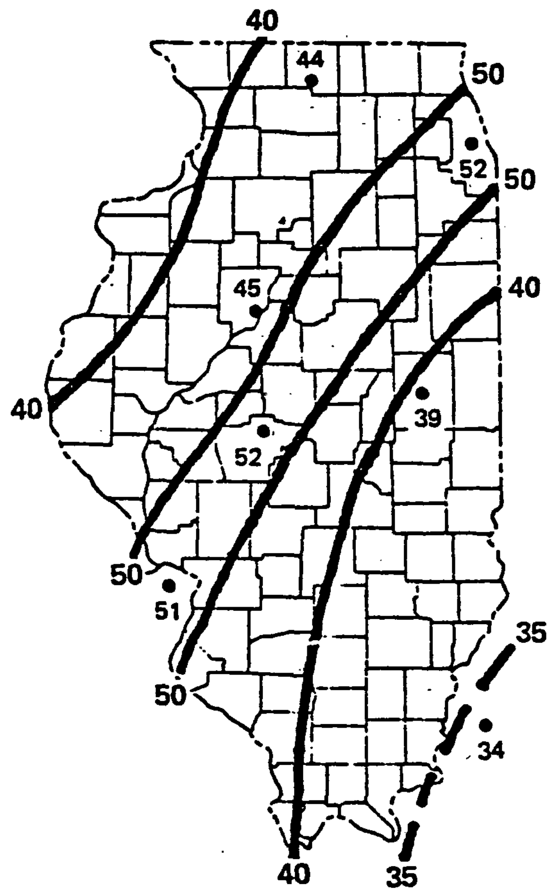

PERCENT OF ALL HOURS
WHEN WINDS ≥10 mph

Figure 16

SOIL TEMPERATURES

The surface of the earth is the zone of most significant energy and mass exchange, and since it also provides the main living space for man, is of great importance to him. Disregarding any plant or man-made cover, the soil of the terrestrial regions of the globe in general acts as a heat sink during summer and daylight hours, and as a heat source during winter and night hours. Consequently, it has the capacity to act as a temperature moderator for living environments, thereby reducing the impact of the customary wide variations in weather over relatively short periods of time, and has the potential to be an important ingredient in an effective energy program.

Factors Affecting Soil Temperature

The soil temperature (T_S) at any given location depends mainly upon the depth of consideration, the nature of the soil, the soil moisture content, slope and aspect of the surface, topography, the nature of the ground surface cover, the absorbed fraction of the incident solar radiation, and the other factors of the energy balance at the soil surface (advection and latent heat exchanges, air temperature, difference between soil surface and air temperatures).

Soil Temperature Variations with Depth

Except for the upper few millimeters and at considerable depth, soil temperatures exhibit the same type of diurnal and annual variations as observed for air temperatures, but with a much more damped response to solar forcing. As a result its observed values remain much steadier than those of related atmospheric parameters, and free of short time scale variability imposed by exchanges in the turbulent atmosphere. In general, soil temperatures at greater depth in Illinois reveal less diurnal and seasonal variation than those at more shallow depths, and are lower in summer or during the day, and are warmer in winter or during the night. Also their near sinusoidal variation patterns exhibit greater temporal lag in maxima and minima with depth.

On a diurnal basis, as the surface temperature increases during the daylight hours, soil temperature tends to increase with depth, resulting in a heat flow down into the soil, while during the night hours the surface cools and soil temperatures tend to increase with depth, resulting in an upwards heat flow. Considered on a seasonal basis the same type of situation exists; with a downwards heat flow during summer and an upwards heat flow during winter. Thus, at any given time the actual vertical heat flow (G) for a slab of soil (of thickness ΔZ) is the resultant of these two. flows, and is given as:

$$G = -k_s \frac{\Delta T_s}{\Delta Z}$$

where ΔA_S is the change in temperature over the depth ΔZ. The term k_s is called the thermal conductivity, or the ability of the soil to transport heat; its value depends upon the nature of the soil (peat < clay < silt < sand) and also increases approximately logarithmically with increase in soil moisture content. Conventionally the negative sign is given in the equation so that heat flow downwards becomes positive. Table 11 below gives typical values of k_s, and C_s the heat capacity, for three soil types permitting estimates to be made of both heat conductance through the soil profile and heat storage within it.

Table 11. Values of k_s (BTU h^{-1} ft^{-1} $°F^{-1}$) and C_s (BTU ft^{-3} $°F^{-1}$) after van Wijk and de Vries (1963).

Soil Type	Porosity (%)	Moisture Status	k_s	C_s
Sand	40	dry	0.17	19.1
		saturated	1.27	44.1
Clay	40	dry	0.14	21.2
		saturated	0.91	46.2
Peat	80	dry	0.04	8.7
		saturated	0.29	59.9

Typically, for Illinois soils the pattern of diurnal variation is damped out by 0.75 to 1.25 meters, while the annual variation remains evident to about ten times that depth. Little observational evidence is available, but Figure 17 provides mean monthly data for a number of depths in soils on the Agronomy South Farm, Urbana over several intervals of a few years between 1897 and 1963. Since the records were discontinuous over time for any one depth, measured during different time periods for different depths, and available only for Urbana, they have been reduced to monthly means for comparison. They do, however, provide a reasonable indication of the changes in soil temperature with depth in Illinois, and clearly illustrate the reduction in variability and the increasing lag with depth. Table 12 gives the maximum and minimum monthly means, the annual means and the months of warmest and coolest soil temperatures at 8 depths at Urbana. Calculations based upon these data suggest that the maximum and minimum mean monthly soil temperature values for depths of 10, 15, and 20 feet are as provided in Table 13.

There can be considerable variation between different soils and even at different times in the one soil from this average picture of variation in

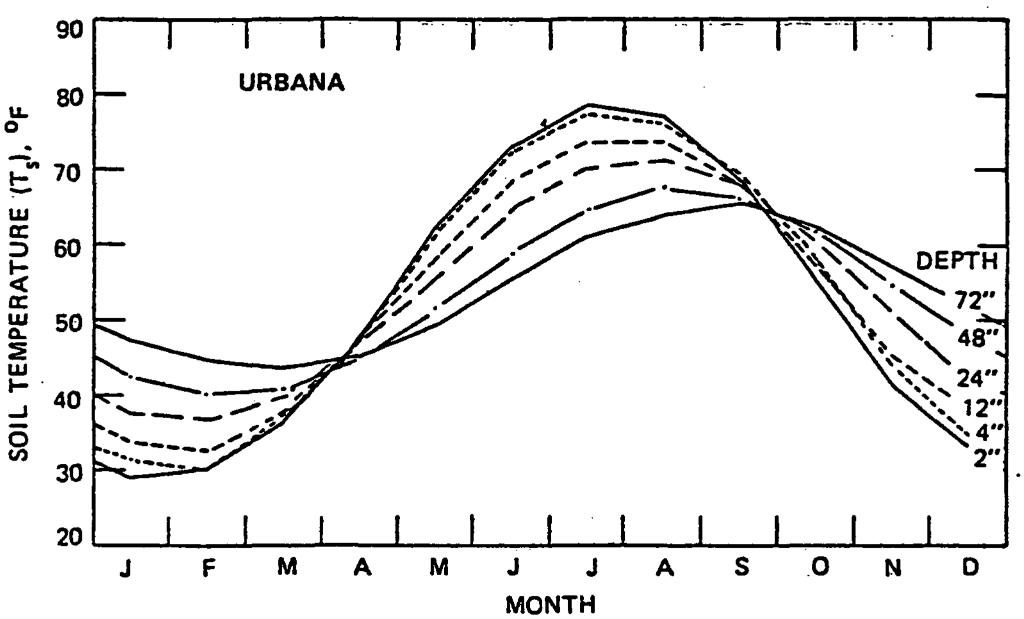
URBANA
SOIL TEMPERATURE (T_s), °F
90
80
70
60
50
40
30
20
J
F
M
A
M
J
J
A
S
O
N
D
MONTH
DEPTH
72"
48"
24"
12"
4"
2"

Figure 17

Table 12. Maximum and minimum monthly means, annual mean range, annual mean, and warmest and coolest months for Urbana soil temperatures. (Mainly after Changnon, 1959.)

Depth (ins)	Min (F)	Max (F)	Range (F)	Mean (F)	Coolest Months	Warmest Months
2	28.9	78.9	50.0	52.9	D,J,F	J,J,A
4	30.1	77.3	47.2	53.0	D,J,F	J,J,A
8	30.6	76.9	46.3	52.3	D,J,F,M	J,J,A,S
12	32.6	73.9	41.3	53.0	D,J,F,M	J,J,A,S
24	36.6	71.4	34.8	53.9	J,F,M	J,A,S
36	38.7	68.9	30.2	53.5	J,F,M	J,A,S
48	40.1	67.8	27.7	53.7	J,F,M,A	J,A,S,0
72	43.6	65.6	22.0	54.0	F,M,A	A,S,0

Table 13. Estimated maximum and minimum mean monthly soil temperatures for Urbana.

Depth (ft)	Min (F)	Max (F)
10	47	61
15	50	58
20	52	54

soil temperature with depth, particularly in the upper 1 meter or so. The factors which influence this variation are the composition and porosity of the soil, the soil moisture content, and the nature of the surface cover. The influence of the surface cover will be discussed in the next sub-section. The composition of the soil and its porosity influence its thermal conductivity or ability to transfer heat (see Table 11) and its heat capacity. The soil moisture content of the soil also affects its thermal conductivity (see Table 11) and heat capacity. As the soil moisture content increases the heat capacity increases approximately linearly thereby reducing variability, while the thermal conductivity increases approximately logarithmically, thereby increasing conductance and hence responsiveness. Thus, the effects of composition, porosity and soil moisture interplay to govern the vertical flow of heat up or down, so influencing the final temperature profile.'

Energy Receipt/Loss at the Soil Surface

The receipt or loss of energy at the soil surface results in a change in soil surface temperature, which alters the thermal gradient with depth, and provides the driving force for a change in the cascade of heat down through the soil profile, or in its transfer upwards in the manner outlined above. These surface exchanges are controlled largely by the net radiation (net solar and infrared radiant energy) at the soil surface. The prime forcing function determining the net radiation during daylight hours is the absorbed fraction of the incident solar radiation, while during nighttime exchanges of the longer wavelength infrared radiant energy between the atmosphere and the surface dominate. Other heat exchange processes, namely the advection of heat to or from the area by the atmosphere, and/or the gain/loss

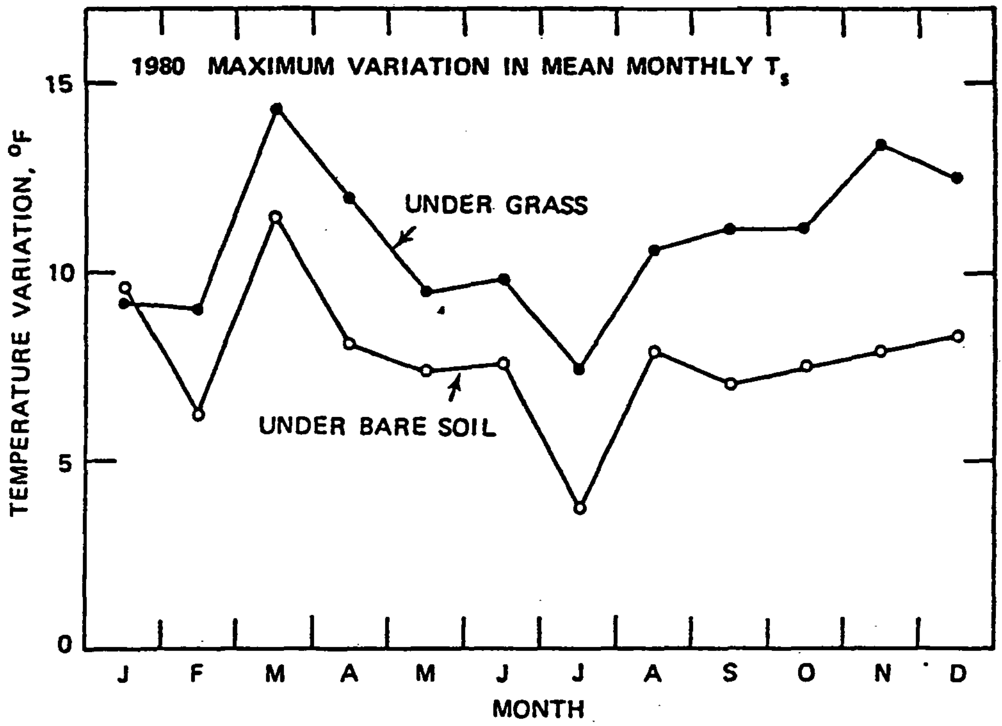
1980 MAXIMUM VARIATION IN MEAN MONTHLY T_s
15
10
5
0
TEMPERATURE VARIATION, °F
UNDER GRASS
UNDER BARE SOIL
J
F
M
A
M
J
J
A
S
O
N
D
MONTH

Figure 18

of latent heat of vaporization during condensation/evaporation at the surface, can either supplement or be supported by the net radiation to give the full energy balance.

This picture of energy exchange is made more complex by a number of factors, including the diurnal and seasonal patterns of incident solar energy at any point, the latitudinal variation in receipt of solar radiation, cloudiness (and hence climate) and other atmospheric aerosols, the degree of slope and the aspect of the surface, local topography, the nature of the soil surface and its moisture content, and the nature of any surface cover. The variations and spatial and temporal patterns of a number of these factors have been considered in other sections, and so will be given only cursory treatment here.

Figure 18 illustrates the impact of the latitudinal variation of solar radiation receipt upon soil temperatures in Illinois. It provides the maximum variation in mean monthly soil temperatures across the state, with the extremes being from north to south, and hence latitudinal in most cases (see Figs. 21 and 22). This difference is greatest during the period of low solar elevation (except for January and February when snow-cover acts as a moderator) when the latitudinal effect is most marked, being on the order of 1Q-15°F under grass cover, and 8-12°F under bare soil. It is smallest during the summer months of high solar elevation when the latitudinal variation in incident solar energy is least, and is on the order of 7-10°F under grass cover and 4-7°F under bare soil. Figure 19 illustrates the typical annual pattern of soil temperature at a shallow depth (4 inches) for a central Illinois site. During January and February an insulating blanket of snow and ice keeps the soil temperature at close to the freezing point despite much lower air temperatures. When air temperatures increase rapidly during March to May soil temperatures at shallow depths also increase rapidly with the monthly mean values of both parameters remaining very close. For the remainder of the year (June to December) the mean soil temperature exceeded the mean air temperature by 3-6°F.

The nature of the soil surface and its moisture content also influence the energy receipt. The black and dark-gray soils of Illinois offer a low reflectivity to solar radiation, on the order of 5-15%, and being lowest when moist, while the lighter colored soils have a reflectivity in the range of 10-30%, again varying in the same manner with moisture level. Thus for the same solar energy receipt the black soils absorb a greater fraction of the available energy, particularly if moist.

The type of surface cover also influences soil temperatures. In the case of a snow cover, the reflectivity is markedly increased to a value of about 40-90%, dependent upon age of the snow (decreases with age) and depth of the snow (increases with depth to about 20 cm). Thus, a snow cover results in a decrease in solar energy penetrating to the soil and consequently in the amount absorbed as can be inferred from the February data in Figure 20. In the case of a plant cover, conditions are also modified considerably since plants tend to shade the surface, increase organic matter in the upper soil layers, increase porosity of the soil and amend the water flow and storage characteristics. This causes a complex impact upon the surface energy balance, and hence, upon soil temperatures. Figure 19 illustrates the typical reduction in annual range of mean monthly soil temperatures resulting from a grass cover compared to a bare soil with mean summer values of the former being 2-3°F less and mean winter values 2-3°F higher. Figure 20 shows the much more conservative range of soil temperatures at 4 inches (absolute and mean) under a grass cover compared to under bare soil for all months of the year.

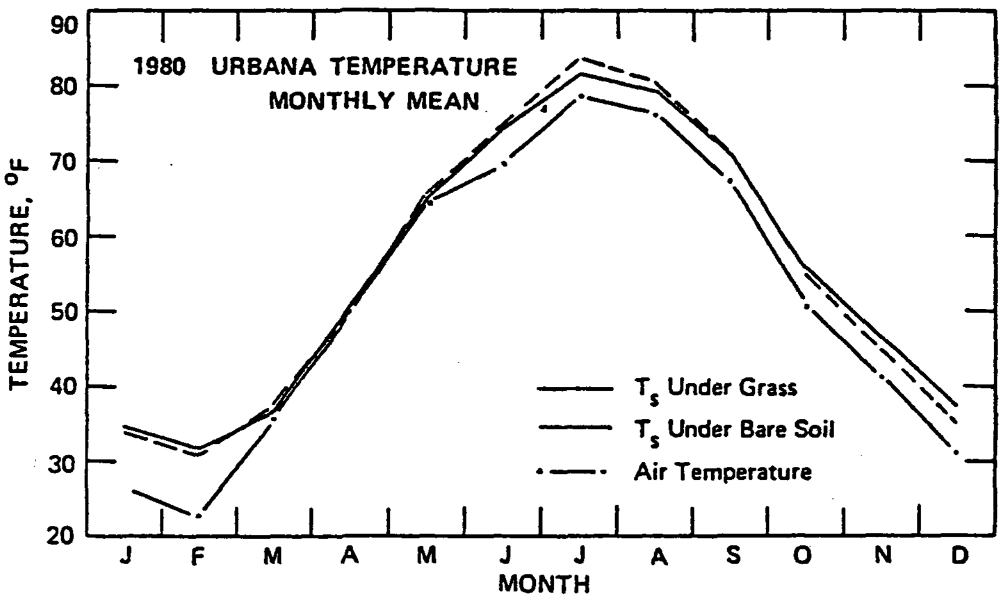
1980 URBANA TEMPERATURE
MONTHLY MEAN
TEMPERATURE, °F
90
80
70
60
50
40
30
20
Ts Under Grass
Ts Under Bare Soil
Air Temperature
J
F
M
A
M
J
J
A
S
O
N
D
MONTH

Figure 19

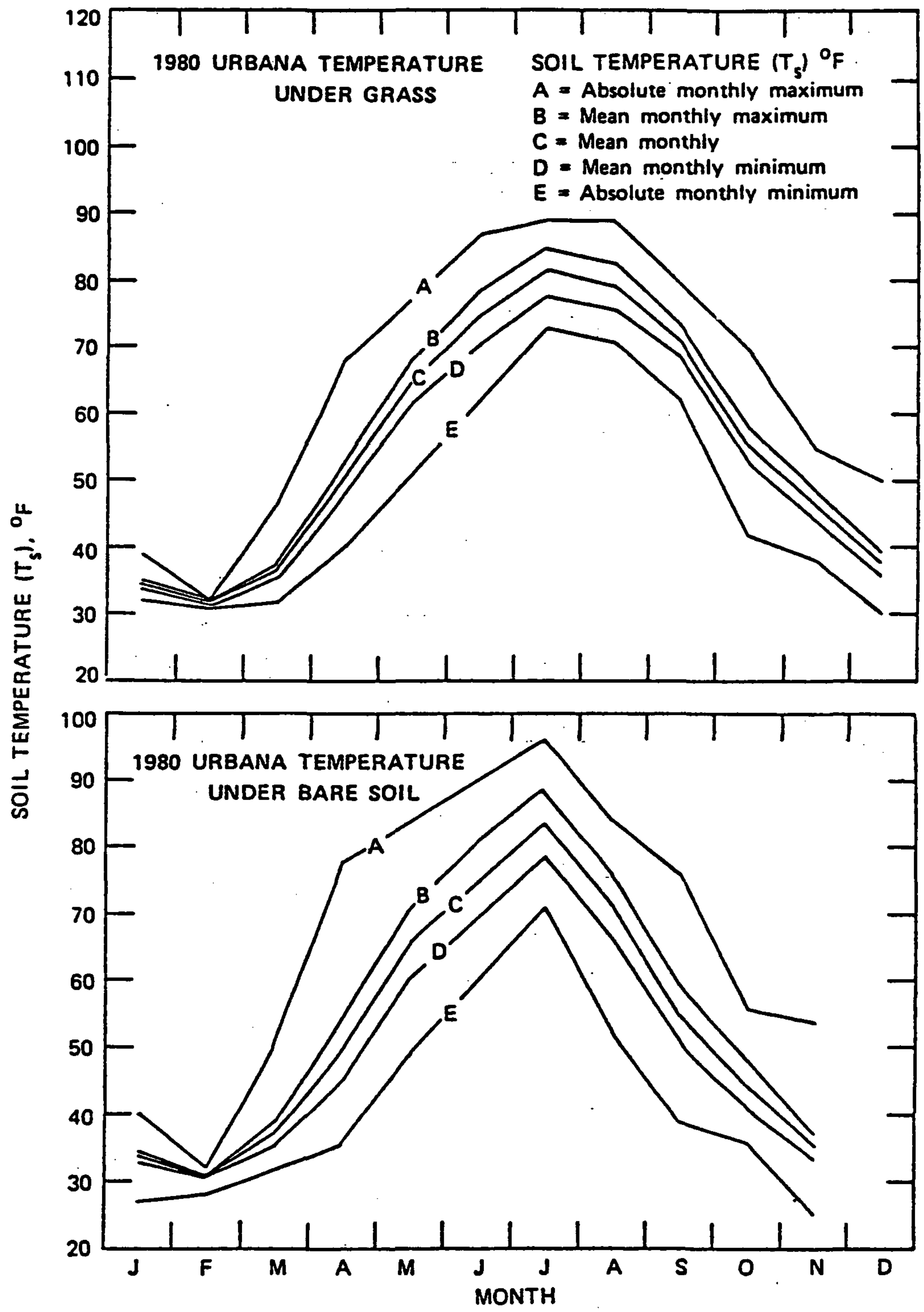
1980 URBANA TEMPERATURE
UNDER GRASS
SOIL TEMPERATURE (T_s) °F
A = Absolute monthly maximum
B = Mean monthly maximum
C = Mean monthly
D = Mean monthly minimum
E = Absolute monthly minimum
1980 URBANA TEMPERATURE
UNDER BARE SOIL
SOIL TEMPERATURE (T_s), °F
J F M A M J J A S O N D
MONTH

Figure 20

Spatial Variation in Soil Temperatures over Illinois

The above discussions of energy receipt/loss at the soil surface and of variations in soil temperature with depth can be used to explain and understand the pattern of soil temperatures observed over the state. Unfortunately there is little spatial information at any consistent depth other than 10 cm (4 inches), and even the state-wide measurement of soil temperature at this depth is a recent undertaking. Thus, it was decided that the following outline of the spatial picture should be based largely upon 1980 data only for 18 stations around the state where soil temperature has been measured at 4 inches under both bare soil and a grass cover. This provides the most complete picture for the data available (most stations, most complete data), but it must be realized that while the relative nature of the month-to-month, areal, and bare soil to grass cover variations is quite good, the absolute values may be quite different from the long-term mean values.

Monthly mean isotherms of soil temperature at 4 inches under bare soil are displayed for the state in Figures 21A and 21B, while Figures 22A and 22B provide comparable patterns for soil temperatures at 4 inches under a grass cover. At all times of the year, and under both surface types, there was a latitudinal gradient of soil temperature, with the warmest soils being in the south and the coolest soils in the north. In addition there is a tendency for central and central-south counties to exhibit warmer temperatures than would be expected by a simple latitudinal model, during all except the coldest months, perhaps related to the darker soil types common in these regions. Another interesting feature is the tendency for cooler soil temperatures to be evident in the region of large rivers and water bodies, particularly during the summer months.

1980 MEAN MONTHLY SOIL TEMPERATURE (°F) AT 4" UNDER BARE SOIL

Figure 21A

1980 MEAN MONTHLY SOIL TEMPERATURE (°F) AT 4"' UNDER BARE SOIL

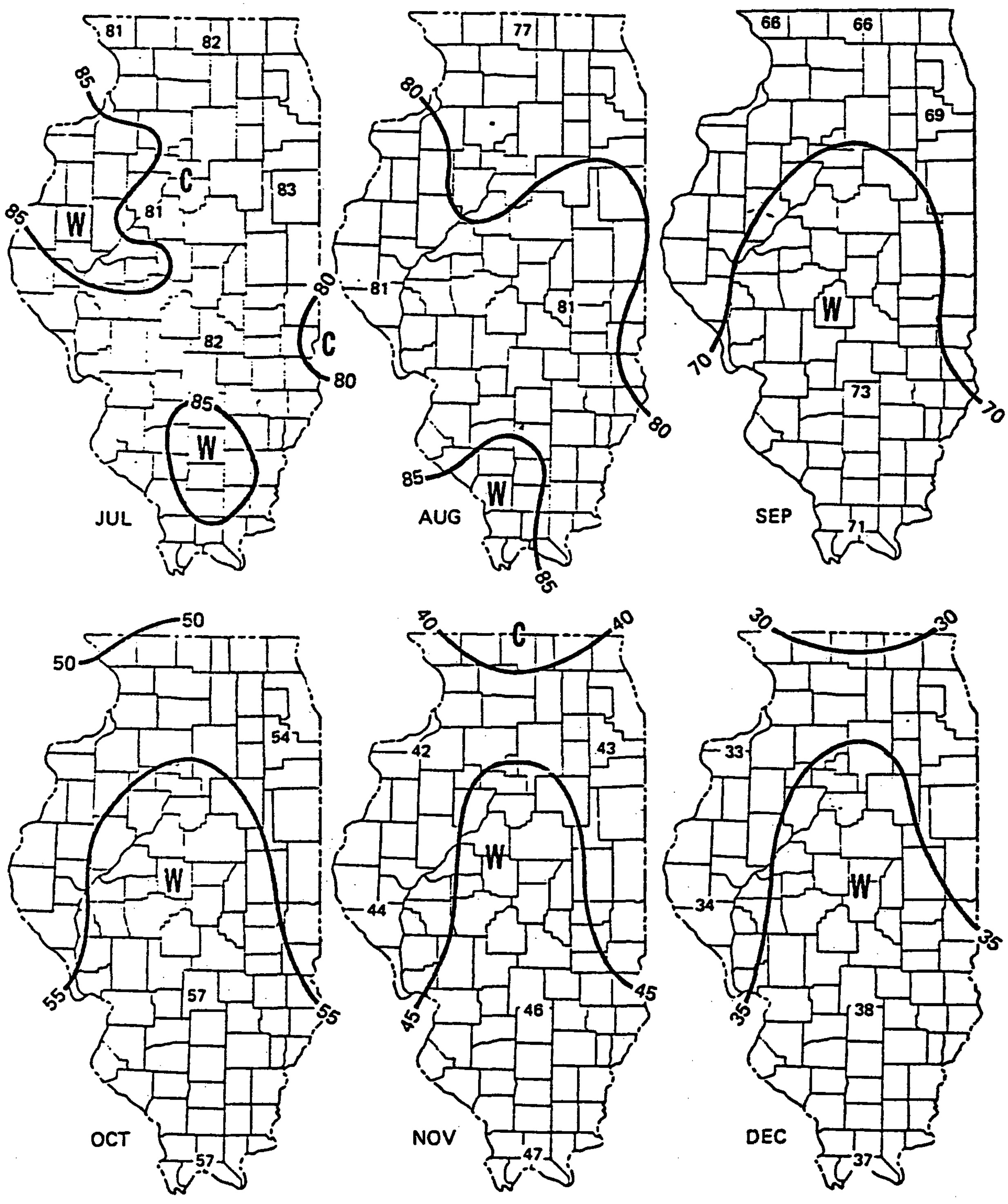

Figure 21B

1980 MEAN MONTHLY SOIL TEMPERATURE (°F) AT 4" UNDER A GRASS COVER

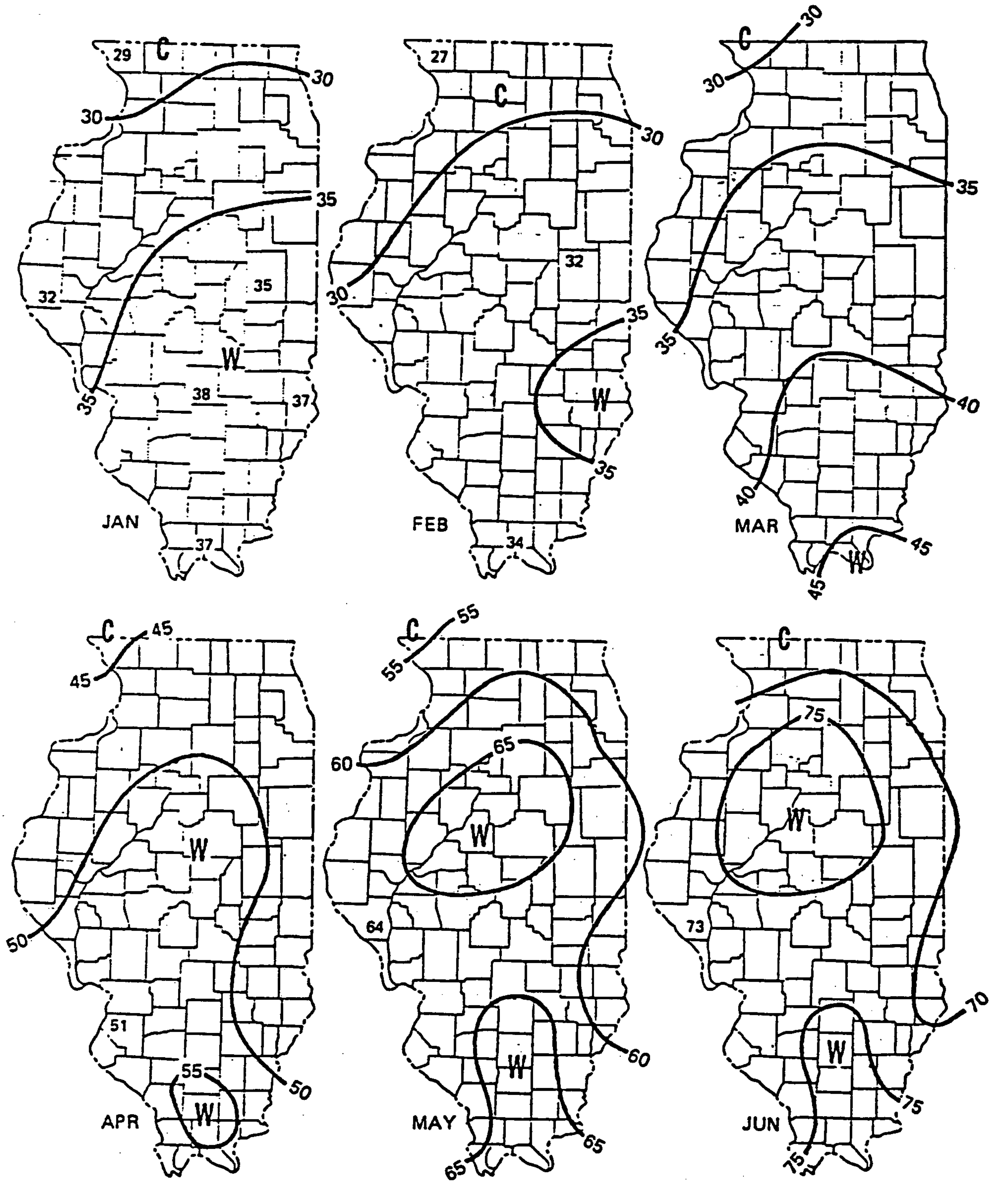

Figure 22A

1980 MEAN MONTHLY SOIL TEMPERATURE (°F) AT 4" UNDER A GRASS COVER

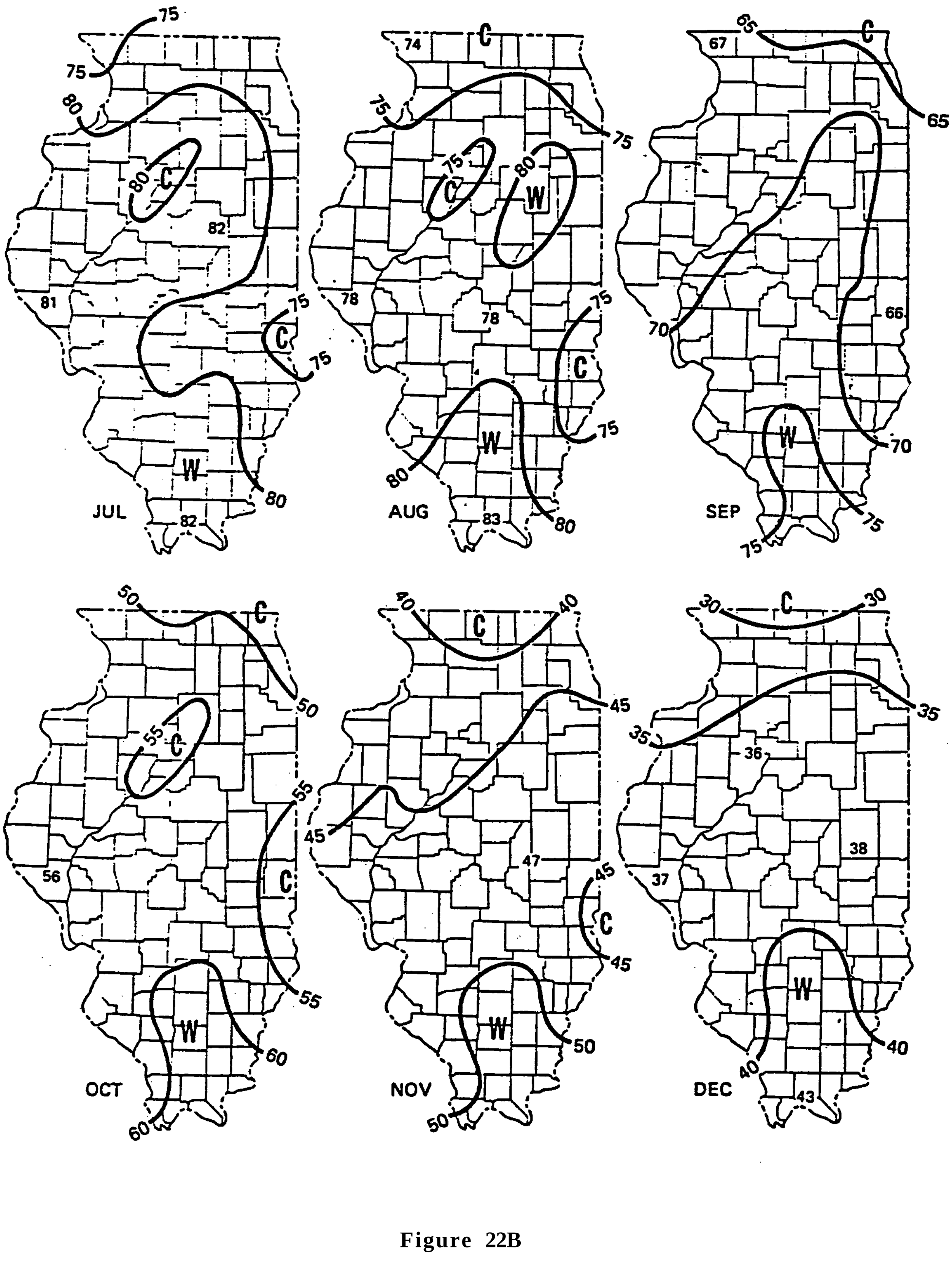

Figure 22B

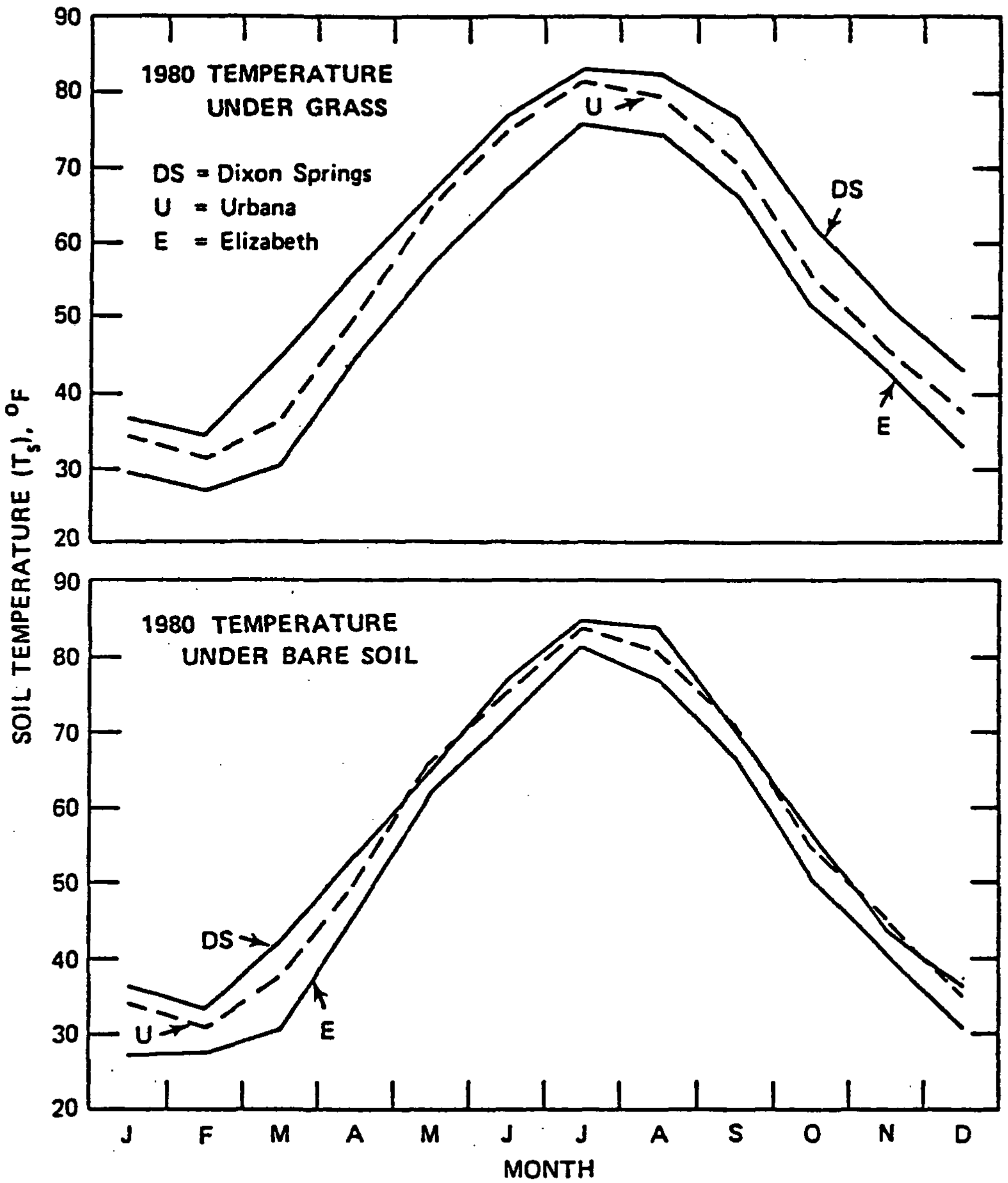
1980 TEMPERATURE
UNDER GRASS
DS = Dixon Springs
U = Urbana
E = Elizabeth
U
DS
E
1980 TEMPERATURE
UNDER BARE SOIL
DS
U
E
SOIL TEMPERATURE (T_s), °F
90
80
70
60
50
40
30
20
J F M A M J J A S O N D
MONTH

Figure 23

The north-south variation in mean monthly soil temperatures is illustrated in Figure 23 which provides data from Dixon Springs (extreme southern), Urbana (east central), and Elizabeth (extreme northwest), while the corresponding annual mean data is given in Table 14 below. These data show clearly than on an annual basis, the mean temperature under bare soil exceeds that under a grass cover in the south, while in the north the reverse is true, and they are very close in the central regions of the state. On a monthly basis, in the south the temperature under grass exceeds that under bare soil in all but the mid-summer months, while in the north temperatures under bare soil tend to be slightly higher from late winter through summer, and intermediate conditions exist in the central counties.

Table 14. Annual mean soil temperatures (°F) at 4 inches under a grass cover and bare soil for Dixon Springs, Urbana, and Elizabeth, 1980.

	Dixon Springs	Urbana	Elizabeth
Under grass cover	59.6	55.2	50.0
Under bare soil	56.8	55.2	50.9

Additionally, while the annual range of soil temperatures under bare soil is close to that under grass, the latitudinal (N-S) variation in monthly means is much greater under grass (typically 1.5-1.7 times) than under bare soil.

References

Changnon, S. A., 1959: Summary of Weather Conditions at Champaign-Urbana, Illinois, SWS, Bull. 47.

van Wijk, W. R., and D. A. de Vries, 1966: Periodic temperature variations in a homogeneous soil. In van Wijk, W. R., (ed), Physics of Plant Environment, North-Holland, Publ. Co., Amsterdam, 102-143.

DEPTH OF FROST DURING WINTER 1980-81

Systematic observations of frost depth have not been made in Illinois until very recently. Any knowledge of frost depth within the state has accumulated from occasional observations that happened to be recorded, or from the experiences of people concerned with frost. The maximum depth that frost penetrates the ground in Illinois is over four feet in the northernmost part of the state, although the absolute maximum depends upon the soil type, moisture concentration, slope and aspect, depth of snow cover, etc., in addition to the severity of the temperature.

The ISWS has initiated a network for systematic observations of frost depth. Members of the Illinois Cemetery Association have volunteered to routinely measure the depth of frost during each month of the winter season, and report to the Water Survey the depth at the end of each month plus the maximum depth observed during the month, snow depth on the ground, vegetation cover and slope and aspect. Results for the first winter are shown in Figure 24. The upper two diagrams represent (a) the frost depth at the end of December 1980, and (b) the maximum frost depth recorded sometime during December. The lower two diagrams (c and d) present similar information for the month of January 1981. Frost depth during the winter of 1980-81 was relatively shallow, undoubtedly due to temperatures being very close to the long-term average and less than normal precipitation in almost all months since July 1980 (particularly in southern Illinois), and therefore less than normal soil moisture. At the end of December, maximum frost depth was only 8 inches in the northwestern part of the state, 2 inches around the Chicago metropolitan area. The southernmost extent of frost was roughly from St. Louis to Salem to Lawrenceville. The maximum depth during the month was only 10 inches in north central Illinois.

During January, the southern frost limit moved south to about St. Louis to Mt. Vernon to about Eldorado. The depth at the end of January varied from slightly greater than 20 inches in northwestern Illinois to about 5-10 inches across the central part of the state. Maximum depth observed during January was slightly greater than 30 inches in the Rockford and Freeport area and about 10 inches in central Illinois. Apparently, there was at least some frost in all counties for at least a short time during January.

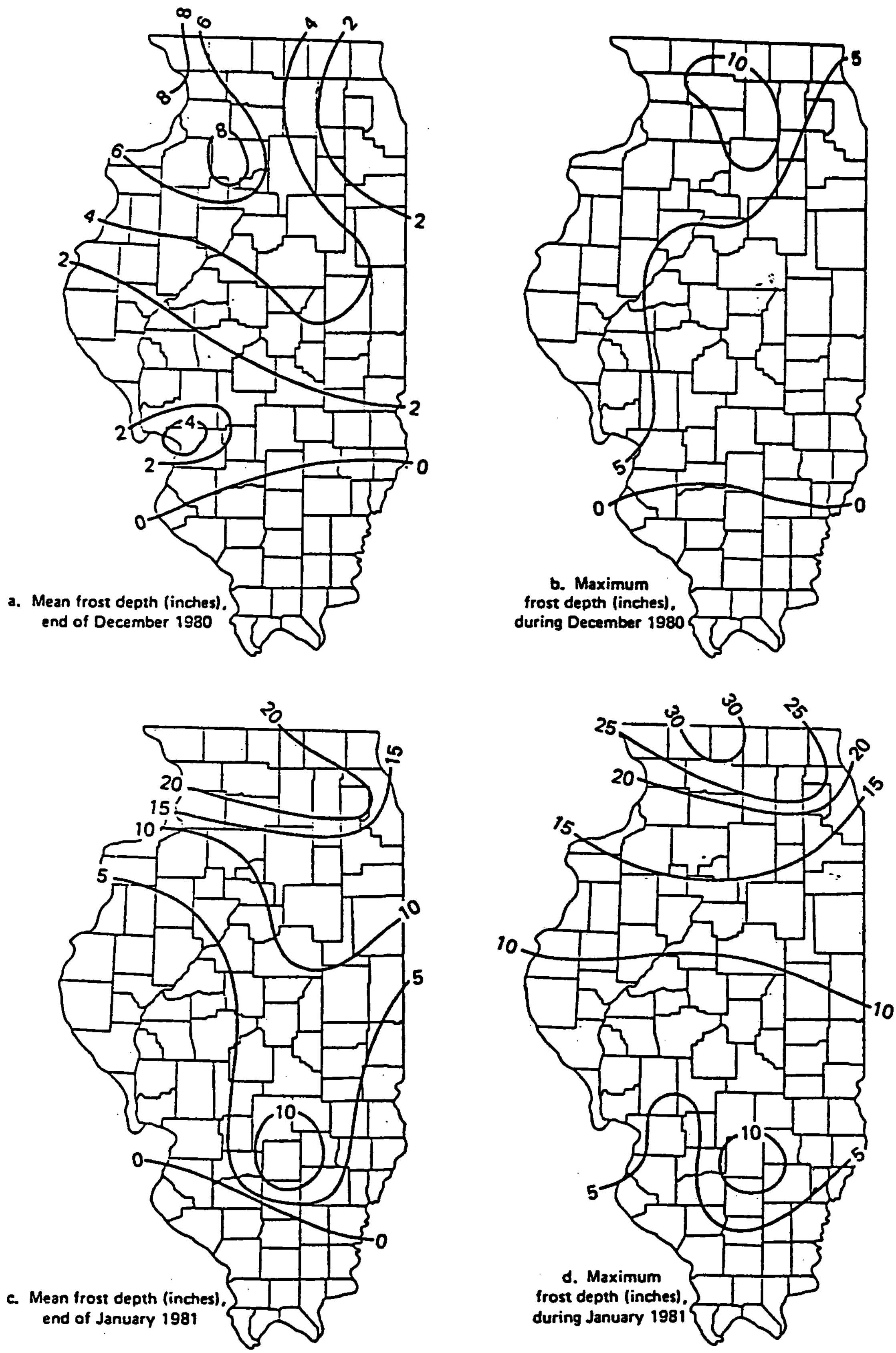

a. Mean frost depth (inches), end of December 1980

b. Maximum frost depth (inches), during December 1980

c. Mean frost depth (inches), end of January 1981

d. Maximum frost depth (inches), during January 1981

Figure 24

WELL WATER TEMPERATURES

Well water has the potential as a heat source as well as sink during winter and summer, respectively, which could be exploited for heating or cooling of residential or business environments. The efficiency of such a system is at least in part dependent upon the difference in temperature of the well water and that of air. Unfortunately, we have no long-term systematic observations of well water temperatures about the State of Illinois. However, well water temperatures change very little with the different seasons of the year (usually limited to a few degrees) and tend to be within a few degrees of the mean annual air temperature at any specific location. Using this criterion, then one would expect well water temperatures in the southern part of Illinois to be about 58°F (15°C), declining to about 48°F (9°C) in the northern part of the state.

FACTORS WHICH IMPACT INSOLATION RECEIVED AT THE EARTH'S SURFACE

Insolation, received at the surface of the earth, depends upon several factors, including the output of the sun, the time of day and year and latitude (which determines solar angle), atmospheric turbidity, and opacity and amount of cloud cover. Given the time of day, date of the year, and latitude of the site, the amount of insolation received at the top of the atmosphere can be calculated very accurately. Attenuation within the atmosphere is much more difficult to derive because it depends upon several variables (e.g., turbidity and cloud opacity and cover). Opacity is difficult to measure and both variables are inadequately known, particularly over poorly populated areas and the oceans.

Although turbidity can be measured, it is not systematically measured or recorded by National Weather Service stations. Rough values can however, be computed as a function of atmospheric temperature, solar angle, humidity, etc. Cloud amount at locations within Illinois which are not regularly monitored by the National Weather Service could be roughly estimated from satellite imagery, although the precision of such studies is severely limited.

FIGURE CAPTIONS

Figure 1A. Illinois monthly means of daily total radiation incident on a horizontal surface (BTU ft^{-2} d^{-1}), January-June.

Figure 1B. Illinois monthly means of daily total solar radiation incident on a horizontal surface (BTU ft^{-2} d^{-1}), July-December.

Figure 2. Illinois annual mean daily total solar radiation incident on a horizontal surface (BTU ft^{-2} d^{-1}).

Figure 3. Monthly mean, extrems and percentile (10th, 25th, 75th, 90th) values of daily total solar radiation received on a horizontal surface at Argonne National Laboratories, Lamont.

Figure 4. The 10th, 25th, 50th, 75th, and 90th percentile values of hourly total incoming solar radiation, partitioned by month for Lamont, IL, after Changnon (1978).

Figure 5. Variations in incoming direct beam and diffuse solar radiation on clear days for Illinois, after Changnon (1978).

Figure 6A. Annual and monthly (February, June, September, December) means of incoming total solar radiation received on a horizontal surface at Lemont, 1950-1978.

Figure 6B. Same as 6A, except for January, March, April, May.

Figure 6C. Same as 6A, except for July, August, October, November.

Figure 7. Regression lines fitting annual and monthly means of total solar radiation incident on a horizontal surface at Lemont, 1950-1978.

Figure 8. Mean monthly air temperature, January through June

Figure 9. Mean monthly air temperature, July through December.

Figure 10. Mean heating degree days, January through June. (Plotted values are hundreds of degree days.)

Figure 11. Mean heating degree days, July through December (Plotted values are hundreds of degree days.)

Figure 12. Mean cooling degree days, May through September. (Plotted values are hundreds of degree days.)

Figure 13. Mean relative humidity at 0600 and 1800, January and April.

Figure 14. Mean relative humidity at 0600 and 1800, July and September.

Figure 15. March of monthly daytime and nighttime percent of hours with wind ≥ 10 mph. Shaded area represents plus and minus one standard deviation from the mean.

Figure 16. Percent of hours during an average year with wind speed at 10 m (33 ft) ≥ 10 mph.